NASA/TM-2011-217182/Volume I
NESC-RP-09-00596

# Comparison of the Booster Interface Temperature in Stainless Steel (SS) V-Channel versus the Aluminum (Al) Y-Channel Primer Chamber Assemblies (PCAs)

*Roberto Garcia/NESC*
*Langley Research Center, Hampton, Virginia*

*Regor L. Saulsberry*
*Whte Sands Test Facility, Las Cruces, New Mexico*

October 2011

**NASA STI Program . . . in Profile**

Since its founding, NASA has been dedicated to the advancement of aeronautics and space science. The NASA scientific and technical information (STI) program plays a key part in helping NASA maintain this important role.

The NASA STI program operates under the auspices of the Agency Chief Information Officer. It collects, organizes, provides for archiving, and disseminates NASA's STI. The NASA STI program provides access to the NASA Aeronautics and Space Database and its public interface, the NASA Technical Report Server, thus providing one of the largest collections of aeronautical and space science STI in the world. Results are published in both non-NASA channels and by NASA in the NASA STI Report Series, which includes the following report types:

- TECHNICAL PUBLICATION. Reports of completed research or a major significant phase of research that present the results of NASA programs and include extensive data or theoretical analysis. Includes compilations of significant scientific and technical data and information deemed to be of continuing reference value. NASA counterpart of peer-reviewed formal professional papers, but having less stringent limitations on manuscript length and extent of graphic presentations.

- TECHNICAL MEMORANDUM. Scientific and technical findings that are preliminary or of specialized interest, e.g., quick release reports, working papers, and bibliographies that contain minimal annotation. Does not contain extensive analysis.

- CONTRACTOR REPORT. Scientific and technical findings by NASA-sponsored contractors and grantees.

- CONFERENCE PUBLICATION. Collected papers from scientific and technical conferences, symposia, seminars, or other meetings sponsored or co-sponsored by NASA.

- SPECIAL PUBLICATION. Scientific, technical, or historical information from NASA programs, projects, and missions, often concerned with subjects having substantial public interest.

- TECHNICAL TRANSLATION. English-language translations of foreign scientific and technical material pertinent to NASA's mission.

Specialized services also include creating custom thesauri, building customized databases, and organizing and publishing research results.

For more information about the NASA STI program, see the following:

- Access the NASA STI program home page at *http://www.sti.nasa.gov*

- E-mail your question via the Internet to help@sti.nasa.gov

- Fax your question to the NASA STI Help Desk at 443-757-5803

- Phone the NASA STI Help Desk at 443-757-5802

- Write to:
  NASA STI Help Desk
  NASA Center for AeroSpace Information
  7115 Standard Drive
  Hanover, MD 21076-1320

NASA/TM-2011-217182/Volume I
NESC-RP-09-00596

# Comparison of the Booster Interface Temperature in Stainless Steel (SS) V-Channel versus the Aluminum (Al) Y-Channel Primer Chamber Assemblies (PCAs)

*Roberto Garcia/NESC*
*Langley Research Center, Hampton, Virginia*

*Regor L. Saulsberry*
*Whte Sands Test Facility, Las Cruces, New Mexico*

National Aeronautics and
Space Administration

Langley Research Center
Hampton, Virginia 23681-2199

October 2011

Available from:

NASA Center for AeroSpace Information
7115 Standard Drive
Hanover, MD 21076-1320
443-757-5802

# Comparison of the Booster Interface Temperature in Stainless Steel (SS) V-Channel versus the Aluminum (Al) Y-Channel Primer Chamber Assemblies (PCAs)

**July 21, 2011**

## Approval and Document Revision History

NOTE: This document was approved at the July 21, 2011, NRB. This document was submitted to the NESC Director on August 22, 2011, for configuration control.

| Approved: | *Original Signature on File* | 8/22/11 |
|---|---|---|
| | NESC Director | Date |

| Version | Description of Revision | Office of Primary Responsibility | Effective Date |
|---|---|---|---|
| 1.0 | Initial Release | Mr. Roberto Garcia, NASA Technical Fellow for Propulsion; Mr. Regor Saulsberry, Pyrotechnic and Propulsion Component Testing, JSC - WSTF | 7/21/11 |

# Table of Contents

## Volume I: Technical Assessment Report

## List of Figures



## List of Tables

## Volume II: Appendices (separate volume)

# Volume I: Technical Assessment Report

## 1.0 Notification and Authorization

Mr. Roberto Garcia, NASA's Technical Fellow for Propulsion, requested a technical assessment of the performance improvement achieved by the introduction of the stainless steel (SS) V-channel compared to the aluminum (Al) Y-channel Primer Chamber Assembly (PCA) design. The SS V-channel PCA was developed for NASA's Mars Science Laboratory (MSL) Project. The principle focus of the assessment was to measure the transient temperature at the booster interface with both designs.

A NASA Engineering and Safety Center (NESC) Technical Assessment was approved at an out-of-board on November 4, 2009. Mr. Regor Saulsberry, at the NASA Johnson Space Center (JSC) - White Sands Test Facility (WSTF), was selected to lead this assessment. The assessment plan was approved by the NESC Review Board (NRB) on November 19, 2009. Version 2.0 of the plan provided additional testing to evaluate the effects of various staggered firing times (skew) and flow path cross-sectional areas. The updated plan was approved on May 27, 2010. A status briefing for Phase I was presented to the NRB on May 6, 2010. The final report was presented for approval on July 21, 2011.

Key stakeholders for this assessment include NASA, NASA contractors, other government agencies, and outside contractors involved in spacecraft fabrication and operations. This includes most space exploration programs such as Space Launch System, the Multi-Purpose Crew Module (MPCV), MSL, Earth observing programs, and commercial spacecraft programs.

# 2.0 Signature Page

Submitted by:

*Team Signature Page on File – 9/26/11*

| | | | |
|---|---|---|---|
| Mr. Roberto Garcia | Date | Mr. Regor L. Saulsberry | Date |

Significant Contributors:

| | | | |
|---|---|---|---|
| Mr. Stephen H. McDougle | Date | Mr. Adam A. Pender | Date |
| Mr. Kenneth L. Johnson | Date | Ms. Asia N. Quince | Date |
| Mr. Anthony D. Carden | Date | Mr. William Sipes | Date |
| Ms. Sandra Verba | Date | | |

Signatories declare the findings and observations compiled in the report are factually based from data extracted from Program/Project documents, contractor reports, and open literature, and/or generated from independently conducted tests, analysis, and inspections.

# 3.0 Team List

| Name | Discipline | Organization |
|---|---|---|
| **Core Team** | | |
| Roberto Garcia | NASA Technical Fellow for Propulsion | MSFC |
| Regor Saulsberry | NESC Assessment Lead | JSC - WSTF |
| Stephen McDougle | Deputy Assessment Lead | MEIT, JSC - WSTF |
| Tony Carden | Electrical Engineer | ERC, Inc., WSTF |
| Ken Johnson | Statistics | MSFC |
| Loutricia Johnson | Program Analyst | LaRC |
| Adam Pender | Propulsion Systems | Lockheed Martin |
| Asia Quince | Pyrotechnics | JSC |
| William Sipes | Pyrotechnics Devices | Jacobs, JSC - WSTF |
| Sandra Verba | Sr. Program Mgr Aerospace/Pyrovalves | Conax Florida Corporation |
| **Consultants** | | |
| Saverio D'Agostino | Materials and Processes | JPL |
| Carl Guernsey | MSL Prop System | JPL |
| Michael Hagopian | Propulsion Systems Components | GSFC |
| Masashi Mizukami | MSL Prop System | JPL |
| Troy Rayner | Senior Propulsion Engineer | Lockheed Martin |
| Steve Rickman | NASA Technical Fellow for Passive Thermal Analysis | JSC |
| Robert Sadenwater | Aerospace Engineering Supervisor - Pyrovalves | Conax Florida Corporation |
| Keith Van Tassel | Pyrotechnic Systems | JSC |
| Richard Webster | Pyrotechnic Systems | JPL |
| Stephen Woods | Propellant Physicist | Jacobs, JSC - WSTF |
| Zachary Zenz | Pyrovalve Design Engineer | Conax Florida Corporation |
| **Administrative Support** | | |
| Tina Dunn-Pittman | Project Coordinator | LaRC/ATK |
| Donna Gilchrist | Planning and Control Analyst | LaRC/ATK |
| Erin Moran | Technical Writer | LaRC/ATK |

## 3.1 Acknowledgements

NESC Resident Engineer, Ms. Courtney Flugstad, is acknowledged for her initial lump mass heating calculations for zirconium potassium perchlorate (ZPP) burning. NESC Resident Engineer, Mr. Brian Anderson, is acknowledged for his investigation of compression heating. Cobham and its subsidiary, Conax Florida Corporation, are acknowledged for their technical support and for providing the SS PCAs used for this assessment.

# 4.0 Executive Summary

In October 2008, the NASA Engineering and Safety Center (NESC) generated a report entitled, Conax Y-PCA (Primer Chamber Assembly) Booster Anomaly Investigation [ref.1]. This report detailed an independent assessment of four spacecraft propulsion system pyrovalve anomalies that occurred during ground testing. In all four cases, the aluminum (Al) PCA featuring a Y-channel and dual NASA Standard Initiators (NSI) was used. In the ground tests, the nearly simultaneous (i.e., separated by less than 20 microseconds (µs)) firing of both initiators failed to ignite the booster charge.

In 2007 as a result of the then ongoing NESC's assessment, the Mars Science Laboratory (MSL) project team decided to modify PCA design in the attempt to minimize the identified weakness of the Al Y-channel PCAs. Two modifications were made: the PCA body was changed from Al to stainless steel (SS) to avoid melting and distortion of the NSI flow passages when the device functioned; and the interconnected flow passages were separated to a V-channel in an effort to more efficiently transfer energy from the NSIs to the booster charge. MSL project development and qualification testing of the SS V-channel PCA design demonstrated improved performance in terms of shorter booster ignition times and greater thermal margin for booster ignition.

However, the 2008 NESC report recommended that the SS V-channel PCA should be experimentally characterized and quantitatively compared to the Al Y-channel PCA design prior to widespread application to NASA programs and project. This NESC assessment is intended to generate this quantitative comparison of the PCA designs.

In the first phase of this assessment, single and dual simultaneous firings of the NSIs were performed in both PCA types to characterize the peak temperature, pressure rise time, and pressure magnitude delivered to the booster membrane/propellant charge interface (i.e., underside of the booster charge cover). The results indicated the SS V-channel PCAs delivered an average maximum booster/propellant interface temperature approximately 600 °F greater than that delivered by the Al Y-channel PCAs. The higher interface temperature was achieved in one-half the rise time (i.e., 776 versus 1,342 µs for the SS V-channel and the Al Y-channel PCAs, respectively). Pressures in the NSI cavity averaged 3,000 psi greater in the SS V-channel than the Al Y-channel PCAs.

Finally, the testing showed that simultaneous (i.e., within 20 µs) NSI firing significantly reduces the performance of either PCA design to the point where it is unlikely that the booster charge would be reliably ignited. This is consistent with findings from previous NESC assessments [ref. 1]. The booster interface temperature needed to ignite the titanium hydride/potassium perchlorate booster charge is approximately 1,000 °F. In some simultaneous test firings the maximum temperature observed was below the lower limit (i.e., 572 °F) that could be detected by the test instrumentation.

The second phase of this assessment evaluated the effects of NSI staggered firing times (skew) and PCA flow passages cross-sectional area of the SS V-channel PCAs. This testing showed that even with flow paths having 4 times the original cross-sectional area, simultaneous (i.e., within

20 μs) NSI firings significantly reduces performance to the point where it is doubtful that the booster charge would be reliably ignited. In addition, the flow paths with enlarged cross-sections (i.e., areas 2 and 4 times greater than the original design) did not consistently produce significantly higher temperatures at the booster interface.

When the flow path diameter and the skew were high, the combined factors exerted a downward effect on peak pressure. The flow paths with cross-sectional areas 2 and 4 times greater than the original design produced lower pressures in the NSI cavity (i.e., about 1,600 psi and 2,400 psi, respectively). This was not unexpected due to the larger free volume with enlarged flow paths. Near-simultaneous firings resulted in lower temperatures and booster charge cover burn-through percentages.

Proof of concept testing of a prototype PCA resonant chamber modification was conducted. However, additional analysis and testing is required to determine if this design feature has the potential to eliminate the requirement for a minimum[1] NSI firing skew time.

Because the assessment did not conduct tests with booster charges, the ability to actuate the pyrovalve was not directly demonstrated. However, the results of this assessment provide spacecraft designers that use pyrovalves with quantitative information regarding PCA selection and reliable use.

In summary, this assessment characterized the SS V-channel PCAs have greater thermal margin for booster ignition and resistance to sidewall burn-through, but has a higher unit weight than the Al Y-channel PCA design. However, Al and SS PCAs will reliably ignite the booster if a minimum NSI firing skew is used. For the SS V-channel PCA design, increasing the flow path diameter with high skew times reduced the maximum pressures inside the PCA, but an insufficient number of tests were conducted to determine with certainty that the peak temperature difference increased with channel diameter.

[1] Minimum NSI firing skew is a function of the design specific pyrovalve firing circuit. Critical factors influencing effective skew include temperature, NSI current, cable length, PCA material.

# 5.0 Assessment Plan

The MSL project is using pyrovalves with SS dual NSI PCAs rather than the more common Al PCAs (see Figure 5.0-1). The SS design with separate flow paths for each NSI appears to address several design shortcomings of the Al PCA with a "Y" shaped flow path. These shortcomings were identified by the NESC's investigation into four failed pyrovalve events [ref. 1]. However, the NESC report recommended the SS PCA design, which appears to offer greater margin towards successful booster charge ignition, should be experimentally-characterized and quantitatively compared to the Al PCA design. This assessment was constructed to provide this quantitative data. In addition to augmenting the MSL project testing, the NESC data will benefit future projects to properly assess the selection and use of the SS V-channel versus the Al Y-channel PCAs.

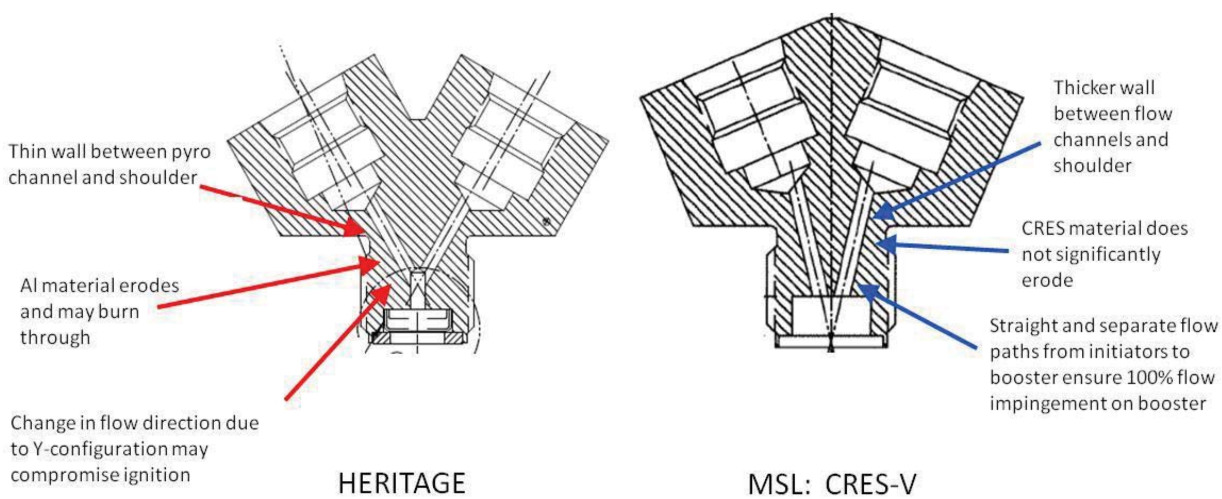


*Figure 5.0-1. Comparison of Al Y-Channel PCA (Heritage) to SS V-Channel PCA (MSL: CRES-V)*

In this two-phased investigation, tests will be conducted to quantify the difference between the two PCA types in ignition temperature delivered to the underside of the booster charge cover (propellant interface). Tests will be performed with single and dual simultaneous NSI firings, varying skew times, and flow path cross section. Testing will use the NESC dual pyrovalve initiator circuit (DPIC) to maintain the skew for simultaneous firings (i.e., within 20 μs) to provide a relative comparison to the NESC Conax Pyrovalve Ignition Failure test data [ref. 1] with the Al PCA design.

Evaluation of the peak temperature and duration on the propellant side of the booster charge cover is a key gauge of the effectiveness of the PCA design in delivering energy from the NSI(s) to the booster charge. By extension, the rapid temperature rise above the booster propellant minimum ignition temperature requirements provides a relative comparison of ignition margin and helps with analysis of valve reliability. This will provide a foundation for more extensive use of the SS PCA dual NSI design on other spacecraft.

# 6.0 Background and Problem Description

## 6.1 Prior Pyrovalves Failures To Ignite Booster Propellant during Ground Testing

In the 2005 and 2006 timeframe, four spacecraft propulsion system pyrovalve failures occurred during ground testing. In all four cases, the nearly simultaneous (skew estimated 5 to 70 μs) firing of dual initiators failed to ignite the booster charge. The Al PCA manufactured by Conax was used. The ZPP combustion products from the dual initiators were directed through a Y-shaped flow channel towards the booster charge. The NESC conducted an independent assessment of these failures [ref. 1].

## 6.2 MSL Project PCA Material and Flow Passage Design Changes

Because the MSL design used a number of mission critical pyrovalves, the MSL project team decided to modify the PCA design to minimize potential anomalies that were associated with the Al PCAs (done in 2006 and 2007). Two key design deficiencies were noted: (1) the PCA Al body material exhibited melting and erosion when the device functioned potentially resulting in decrease of thermal margin and increasing the chance of burn-through; and (2) the interconnected and angled flame passages could be blocked at the intersection. Additional motivation for the design change was provided by the observation that the heritage PCA design often exhibited long (>1 milliseconds (ms)) delays between NSI firing and booster ignition, with booster ignition occurring after the flow within the PCA had ceased.

The MSL project team maintained the flow passage areas, initiator interfaces, and other PCA design attributes not related to the flow path layout. The other proposed changes in the NESC report such as enlarging or shortening the NSI flow passages were not implemented.

The first design modification was to change the body material from 7075 Al to 15-5 SS. The SS material was selected for its strength and higher melting point.

Next, the flow passages were separated into a “V-channel” configuration to provide independent flow passages from the initiator ports to the booster cavity. This approach ensures the initiator combustion products are directed to the top of the booster charge before they can flow to the other (unfired) initiator port. The flow towards the unfired initiator port was shown in the Y-channel design to divert a significant portion of the overall flow. This “bypass” flow and erosion/melting of the Al passage walls at the junction resulted in a significant heat transfer loss.

The internal, open volume of the V-channel PCA was maintained equal to that of the Y-channel PCA so that the initiators would produce the same pressure effects. This was judged to be important because the booster charge output is intended to drive the pyrovalve ram and not to flow back into the initiator cavities.

## 6.3 MSL Project SS V-Channel PCA Testing

The initial testing of the SS V-channel PCAs was identified as *development tests,* as shown in Figure 6.3-1. For these tests, the PCAs were instrumented with pressure transducers in the initiator ports and in a fixture attached to the PCA outlet. This fixture had a 0.122-cubic-inch internal volume to simulate the volume of a pyrovalve piston in the post-stroke condition. There were 37 development tests performed covering a range of temperatures, initiator skew times, and booster charge. Initiators with 70, 100, and 120 percent of the nominal propellant load were used to establish booster ignition thermal margin. The development tests included nine tests of the Al Y-channel PCA design and 28 tests of the CRES-V design. The tests, using the heritage design, with the same test equipment and lot of initiators, validated the test set-up.

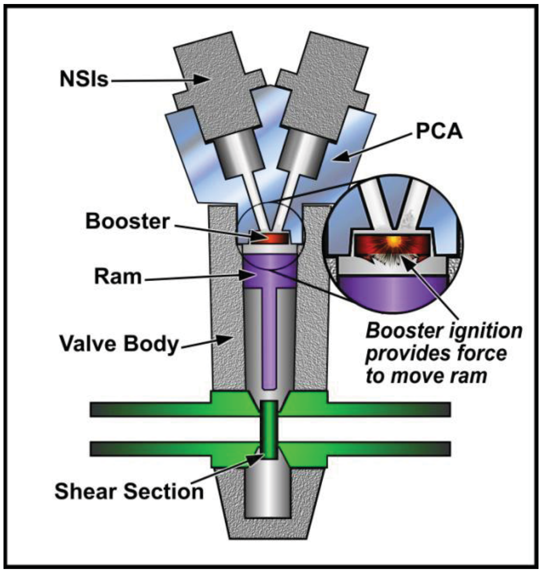


*Figure 6.3-1. Typical SS V-Channel PCA Pyrovalve*

In all of the development tests, the SS V-channel PCAs held an advantage in booster ignition as shown by shorter ignition times which were inferred to mean greater ignition with initiator loads that were as low as70 percent of nominal.

After the successful completion of the development testing, the MSL project team proceeded into qualification testing. To qualify the design, 80, 100, and 120 percent initiators were tested in two different V-channel PCA size configurations at temperatures ranging from -31 to 158 °F. All 40 (20 for each valve size) firings were successful, confirming the shorter booster ignition times and improvements over the heritage design consistent with those observed during the development tests.

Finally, the SS V-channel PCAs were tested on assembled pyrovalves. The ¾-inch pyrovalve qualification phase included 27 fired units, while the 3/8-inch pyrovalve was subjected to a 9-unit delta qualification test. In all cases, the V-channel PCAs met requirements. Four additional PCAs were actuated in ground test unit pyrovalves, bringing the total number of actuations to 106 for the MSL-specific testing.

The MSL-specific PCA testing is documented in Conax TR-397, "Closed Bomb Qualification Test Report, Stainless Steel PCA's for Primer Chamber Assemblies," dated July 11, 2007.

## 6.4 Limitations of the SS V-Channel PCA Design

The SS V-channel PCA design met the intended objectives of the MSL testing, but it did not eliminate the possibility of flow stagnation during simultaneous initiator firings and subsequent failure to ignite the booster charge. Therefore, an operational constraint of firing with a minimum skew of 16 ms was specified for the MSL pyrovalves, with margin tests demonstrating ignition capability/margin with NSI skew times of 8 ms.

Although the SS V-channel PCA design was qualified for use in the MSL project, improvements in temperature and pressure delivered to the booster interface were not quantified.

## 6.5 NESC Testing – Test Apparatus

The Al Y-PCAs used for this project are detailed in Conax drawing number 1125-289-mi. These are the -03 size. The SS V-PCAs used are documented on Conax drawing number 1125-311-C1. These are the -04 size.

All phases of the test project used a sapphire window arrangement in the booster location. The configuration is shown in Figures 6.5-1 and 6.5-2. The test apparatus consisted of a sealing ring, a booster charge cover simulator (0.003-in thick SS membrane), the sapphire window, and a spacer ring. The parts were held in place by a retaining nut on the bottom of the PCA.

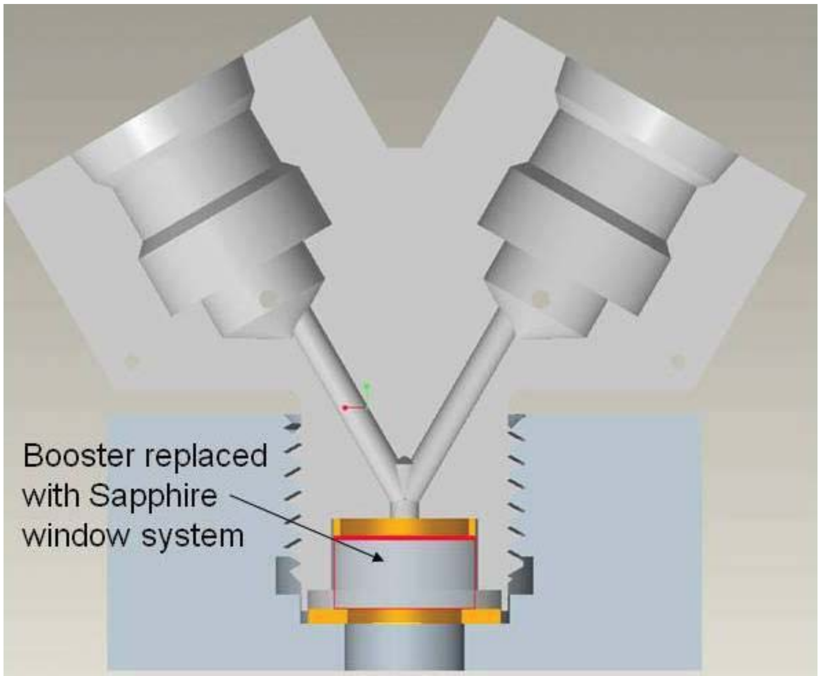


*Figure 6.5-1. Sapphire Window Interface Simulating the Booster Container showing a Al Y-Channel PCA*

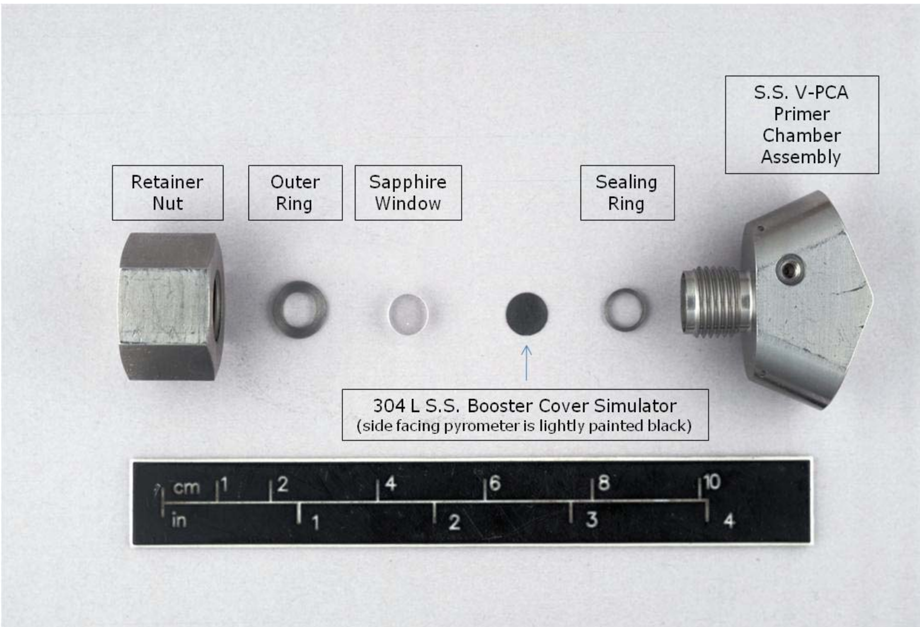


*Figure 6.5-2. Sapphire Window System Parts showing a SS V-Channel PCA*

The booster charge cover simulator was made from 304L, supplied by Caran Precision, Inc., who produce the booster container. Before test, one side of the booster charge cover simulators were coated with flat black paint to provide a consistent emissivity. The coated-side was oriented toward the infrared (IR) pyrometer.

The sapphire window was chosen because of its excellent transmissivity in the IR range. A 4-percent loss across the window was estimated. As the same sapphire window material was used in all tests, the energy loss was a constant (see Figure 6.5-3).

The sealing ring (see Figure 6.5-4) was made from either 17-4PH or 15-5PH SS. Concentric rings were cut in faces to make a labyrinth seal between the sapphire window and the PCA. The sealing arrangement was successfully hydrotested to 30,000 pounds per square inch gauge (psig) with no detectable leakage.

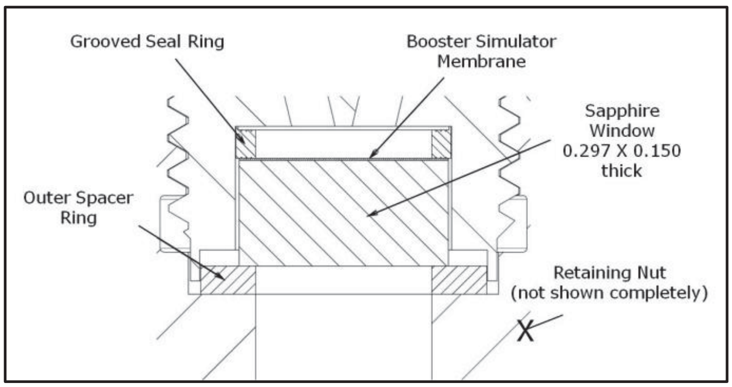


***Figure 6.5-3. Sapphire Window Assembly (dimensions in inches)***

***Figure 6.5-4. Sealing Rings Shown Alongside a U.S. Dime***

One pressure sense port for each NSI cavity was provided in the side of the PCA. The ports were made to accommodate Kistler model 603B1 pressure transducers. The ports were filled with Dow Corning 33 silicone grease to occupy the volume added by the transducer port and to protect the pressure sensor from NSI thermal/shock effects.

The IR pyrometer used for the tests was a model MI-KGA740-HS manufactured by Mikron Infrared, Inc. This unit had a temperature range of 572 to 3,632 °F with a nominal response time of 6 µs.

High-speed video was obtained at 20,000 frames per second with a Phantom™ model 12.1 color camera. This configuration allowed evaluation of the transient temperature at the underside of the booster charge cover, which is normally in contact with the booster propellant.

### 6.5.1 Test Article Mounting and Alignment Fixture

The test article mounting fixture consists of a precision three axis translation stage with a custom machined test article mounting assembly affixed to the upper (Y) stage. The entire assembly is rigidly mounted to the test bed. The assembly provides precision alignment capability for the high-speed pyrometer and is shown with a PCA test article assembly in Figure 6.5-5.

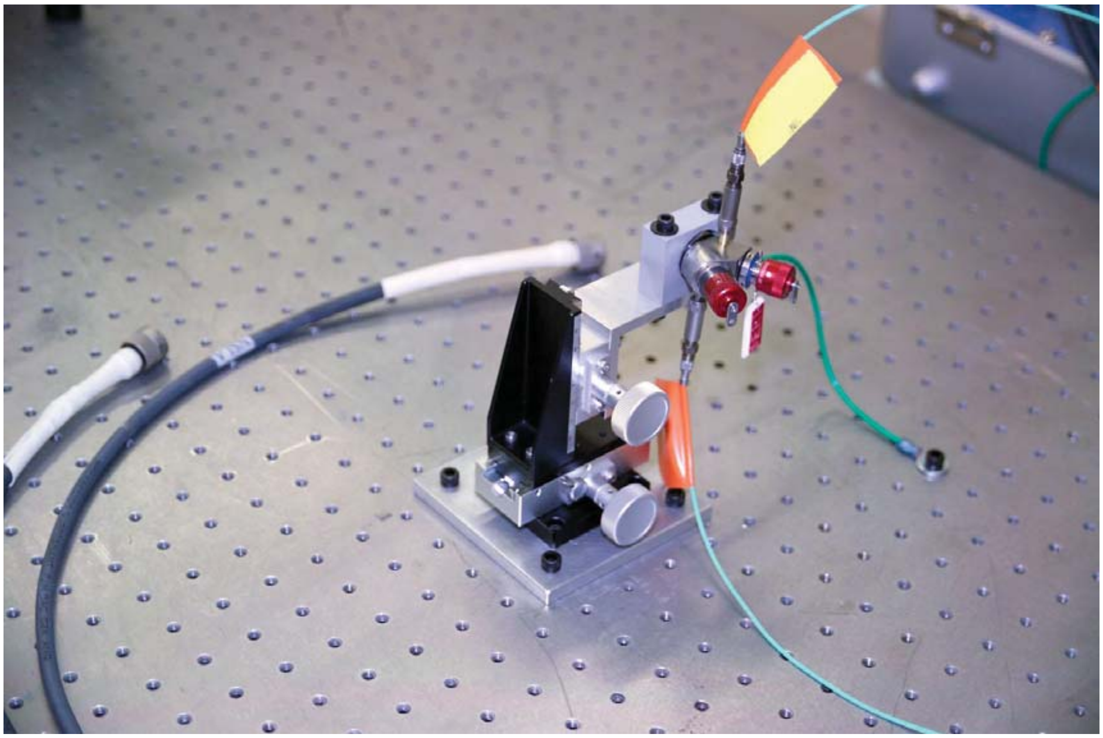

*Figure 6.5-5. PCA Test Article Mounting and Alignment Fixture*

### 6.5.2 NSI Firing Systems

During the course of NESC testing, two NSI firing systems were utilized. Both systems provide high current, approximately 22.5 amps to the NSIs. Normal firing current for the NSIs is usually in the range of 3 to 5 amps. The higher current was used in this project to reduce variations in firings times. These two systems are discussed in the following sections.

### 6.5.3 Kennedy Space Center (KSC) DPIC

This firing system (Figure 6.5-6) was designed for the NESC and built by KSC in July 2006, and was designed to fire the two NSIs simultaneously. The NSIs are connected in series. The system provides outputs for current and voltage monitoring, data acquisition, and camera systems triggering. It is controlled remotely with an arm/fire pendant which contains the safe/arm key switch, firing button, and indicator light emitting diodes.

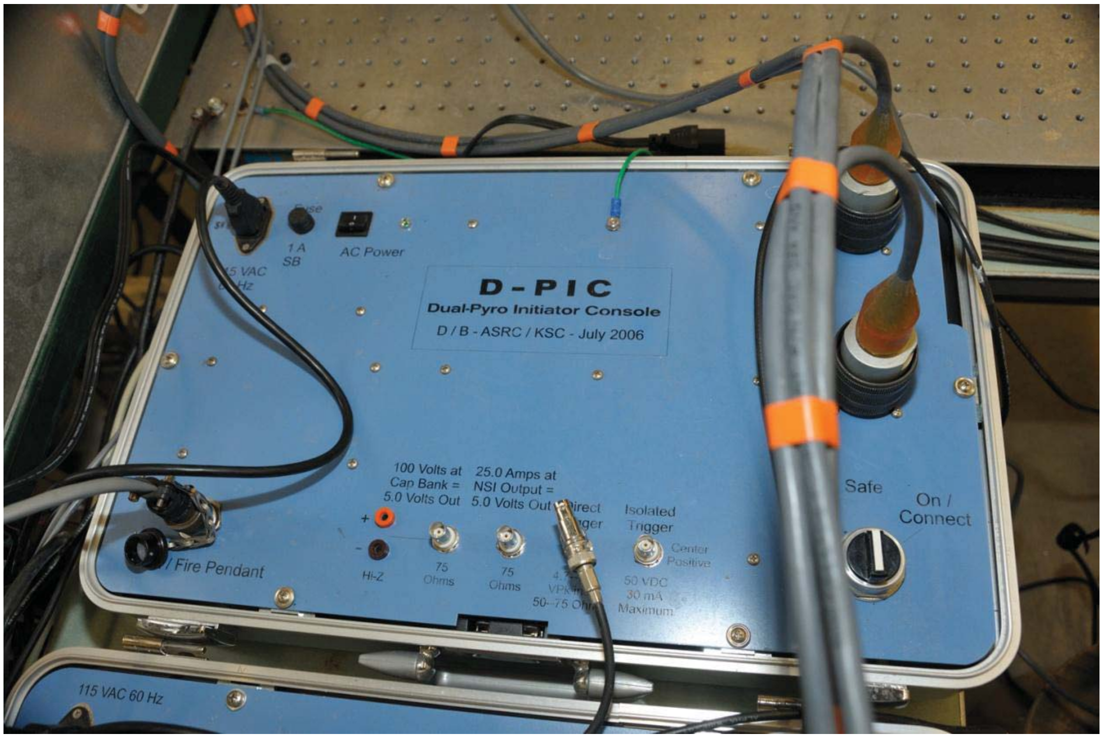


*Figure 6.5-6. KSC DPIC*

### 6.5.4 JSC - WSTF Dual NSI Initiator Set

For Phases IIA and B of the test program, JSC - WSTF designed and built a dual NSI firing system with variable skew capability (Figure 6.5-7). The circuitry for this system was modeled on the KSC DPIC system and designed using information in Johnson Space Center (JSC) 28596A, *NASA Standard Initiator User's Guide.* Both the KSC and WSTF systems utilize capacitive discharge type firing circuits as recommended by JSC-28596A. The fundamental differences between the KSC and WSTF systems are summarized in Table 6.5-1.

***Table 6.5-1. Comparison of KSC DPIC and JSC – WSTF Dual NSI Initiator Set***

| | **KSC DPIC** | **JSC – WSTF Dual NSI Initiator Set** |
|---|---|---|
| **Voltage** (VDC) | 65 | 24 |
| **Firing Circuits/Amperage** (amps) | 1/22.5 | 2/22.5 |
| **Monitoring** | None | NSI current, and data acquisition and high-speed camera triggering |
| **Control** | Manual | Computer |


*Figure 6.5-7. WSTF Dual NSI Initiator Set*

## 6.6 Data Acquisition and Control System

The data acquisition and control system (Figure 6.6-1) consists of a National Instruments PXI (PCI Extension for Instrumentation) chassis with one National Instruments NI PXI-5105 8-channel high-speed digitizer for capturing high-speed transients, and one NI PXI-6229 multifunction data acquisition and control card for firing system control. The data acquisition and control system is capable of simultaneous sampling rates of up to 60 MHz (60 million samples per second) and is fully configurable using the JSC-WSTF software package. The software package was written in C language and was validated before testing began.

For NSI port pressure measures, two each Kistler model 603B1 charge mode pressure transducers with Kistler model 5010 charge amps were utilized. All PCA test articles were machined to accept one pressure transducer in each NSI port. The transducers were installed using a Kistler model 222P needle probe adapter in each port, and protected by the Dow Corning 33 silicone grease.

*Figure 6.6-1. JSC - WSTF Data Acquisition and Control System*

## 6.7 Phase I Testing

All tests were performed at ambient test cell temperatures approximately 60 to 75 °F.

The original test plan for Phase I identified 16 test firings to be performed in the order shown in Table 6.7-1. See Appendix F for discussion of the approach used to design the Phase I test matrix.

*Table 6.7-1. Modified Phase I Test Matrix*

| Run No. | PCA Type | Single or Dual NSI Test | Comment |
|---|---|---|---|
| 1 | Al | Dual | |
| 2 | SS | Single | |
| 3 | Al | Single | |
| 4 | Al | Single | |
| 5 | Al | Dual | Not Performed[1] |
| 6 | SS | Dual | |
| 7 | SS | Single | |
| 8 | Al | Single | |
| 9 | Al | Single | |
| 9B | Al | Single | Repeated Test[2] |
| 10 | Al | Dual | Not Performed[1] |
| 11 | Al | Dual | Not Performed[1] |
| 12 | SS | Dual | Not Performed[1] |
| 13 | SS | Dual | Not Performed[1] |
| 14 | SS | Single | |
| 15 | SS | Single | |
| 16 | SS | Dual | Not Performed[1] |

[1]Because of the test results and the recommendation to proceed with a second phase of testing, test matrix was reduced to 10 test firings.

[2]One of the tests with an Al Y-channel PCA was repeated due to concerns with potential seal leakage, so there were a total of 11 test firings.

See Appendix G for a thorough discussion of the approach used to design the test matrix for Phase I.

## 6.8 Phase II Testing

### Phase IIA

In Phase IIA, the flow passages of select SS V-channel PCAs used in Phase I testing were planned to be enlarged to determine if the larger flow cross-sectional area results in higher temperatures at the booster interface. These trial tests were single NSI firings. The original plan (Figure 6.8-1) called for evaluation of cross-sectional areas 2, 4, 6, and 8 times that of the original flow passage. However, it was recognized that 4 times the original cross-sectional area was the largest that could be accommodated. Dual, simultaneous NSI firings were performed at

4 times the cross-sectional area to determine if this configuration has potential to eliminate the dual simultaneous firing restriction (i.e., minimum skew time) on the PCA.

| Test | Run Order | # NSIs | Skew (µs) | Flow Channel Cross-Sectional Area (Initial = 1) | |
|---|---|---|---|---|---|
| 2 | 4 | 2 | 16,000 | 4 | |
| 4 | 1 | 2 | 16,000 | 2 | |
| 3A | 2 | 2 | 16,000 | 1 | Repeat of Test 3 which had an incorrect skew. |
| 1A | 3 | 2 | 12 | 4 | Repeat of Test 1 which had a cracked sapphire window. |

*Figure 6.8-1. Phase IIA Test Matrix As Performed*

The test matrix was designed to be run in a random order to reduce the effects of uncontrolled variables (e.g., generally, special causes). The actual run order was amended because of the need to correct PCA housing dimensional problems.

A no-fire occurred on the first trial run, which had a skew of 12 µs. This run showed that a larger channel diameter (i.e., 4 times the flow path) would not eliminate the chance of a no-fire. It was decided not to run the remaining 0-skew trials. Three additional trials from the Phase IIA matrix, each at 16,000 µs skew, were completed.

The assessment team did not run enough of the Phase IIA trail tests to be able to say with certainty that the peak temperature difference increased with channel diameter. This question was the basis of the revised Phase IIB test matrix.

**Phase IIB**

After Phase IIA testing was completed, 17 additional tests were planned to further investigate the impact of staggered NSI firings at various area ratios, as shown in Table 6.8-1.

*Table 6.8-1. Original Phase IIB Test Matrix*

| Run Order | Test Article No. | Skew (μs) | Flow Path Cross-Sectional Area Ratio (Initial = 1) |
|---|---|---|---|
| 1 | 10 | 252.5 | 2 |
| 2 | 3 | 500 | 4 |
| 3 | 1 | 500 | 1 |
| 4 | 8 | 500 | 1 |
| 5 | 1 | 252.5 | 2 |
| 6 | 7 | 5 | 1 |
| 7 | 6 | 5 | 1 |
| 8 | 8 | 5 | 2 |
| 9 | 7 | 252.5 | 2 |
| 10 | 10 | 252.5 | 4 |
| 11 | 9 | 252.5 | 1 |
| 12 | 1 | 5 | 4 |
| 13 | 4 | 252.5 | 2 |
| 14 | 8 | 500 | 4 |
| 15 | 7 | 5 | 4 |
| 16 | 5 | 500 | 2 |
| 17 | 2 | 252.5 | 2 |

Phase IIB was designed to determine the relationship between firing skew, flow passage cross-sectional area, booster interface temperature, and the interaction term of skew x area. The test was structured to be able to discern a second-order (quadratic) linear model:

$$Y = \beta_0 + \beta_1 \text{ Skew} + \beta_2 \text{ Area} + \beta_{12} \text{ Skew x Area} + \beta_{11} \text{ Skew}^2 + \beta_{22} \text{ Area}^2$$

where the β's are linear regression parameters fit using the data.

Power was based on the temperature response. The assessment team wanted to observe a difference of 1,000 °F with greater than 80 percent power (~2 standard deviations, based on the Phase I results). The assessment team used design of experiments (DOE) principles to plan the test. An orthogonal matrix ensured that all factors (i.e., β's) would be calculable, with no noise or confounding contributed by other factors. It was desired that the standard error would be constant across the design space, resulting in a good estimate of model parameters and predictions at all points in the domain. The original Phase IIB matrix was randomized to avoid problems with rogue variables.

To avoid thermal and surface roughness effects of re-using previously fired PCAs, it was originally planned that used PCAs would have a larger chamber area before re-use. It was later decided for the 1X flow path area tests to clean used PCAs between runs to minimize the number of units. This resulted in some PCAs being reused 3 times. Following cleaning, PCAs were visually-inspected to verify there was no degradation. Further, an anomalous result happened in the first trial and the trial was re-run using another PCA. An attempt to re-randomize the test sequence for this issue was made, resulting in the updated matrix shown in Table 6.8-2.

***Table 6.8-2. Updated Phase IIB Test Matrix***

| Run Order | Factor 1 A:Skew | Factor 2 **B:Area** | Test Article No. |
|---|---|---|---|
| 1 | 5 | 1 | 3 |
| 2 | 252.5 | 2 | 8 |
| 3 | 500 | 4 | 9 |
| 4 | 500 | 1 | 5 |
| 5 | 500 | 1 | 6 |
| 6 | 252.5 | 2 | 2 |
| 7 | 5 | 1 | 4 |
| 8 | 5 | 2 | 1 |
| 9 | 252.5 | 2 | 2 |
| 10 | 252.5 | 4 | 10 |
| 11 | 252.5 | 1 | 7 |
| 12 | 5 | 4 | 9 |
| 13 | 252.5 | 2 | 1 |
| 14 | 500 | 4 | 10 |
| 15 | 5 | 4 | 9 |
| 16 | 500 | 2 | 8 |
| 17 | 252.5 | 2 | 2 |

If there is an effect of times used, the data is suboptimal to separate that factor from the others. As a lesson learned, it would have been better to design the test blocked on *number of times used*.

# 7.0 Data Analysis

Phase I test data is summarized in Table 7.0-1.

***Table 7.0-1. Phase I Test Data Summary***

**Phase 1 DATA SUMMARY**

| Run | Al - or - SS | Date | Time | Pressure Start Side A (µs) | Max Pressure Side A (psig) | Time Of Max Press Side A (µs) | Pressure Start Side B (µs) | Max Pressure Side B (psig) | Time Of Max Press Side B (µs) | Max Booster Interface Temp (°F) | Time Of Max Temp (µs) | Pressure at 800 µs Side A (psig) | Pressure at 800 µs Side B (psig) | Booster Interface Temp at 800 µs (°F) |
|---|---|---|---|---|---|---|---|---|---|---|---|---|---|---|
| **Single NSI Firings** | | | | | | | | | | | | | | |
| Pre | SS | 02/23/10 | 13:56 | 137 | 11,851 | 151 | 332 | 4,996 | 830 | 2,679 | 716 | 4,777 | 4,840 | 2,669 |
| 2 | SS | 02/24/10 | 12:34 | 140 | 10,926 | 156 | 255 | 4,570 | 824 | 2,823 | 835 | 4,638 | 4,527 | 2,836 |
| 7 | SS | 02/25/10 | 9:40 | 147 | 10,781 | 166 | 324 | 4,996 | 787 | 1,967 | 821 | 4,933 | 4,979 | 1,957 |
| 14 | SS | 02/25/10 | 13:41 | 144 | 10,436 | 159 | 314 | 4,441 | 870 | 1,885 | 726 | 4,690 | 4,232 | 1,842 |
| 15 | SS | 02/25/10 | 14:55 | 147 | 11,085 | 169 | 259 | 4,805 | 845 | 2,485 | 721 | 4,811 | 4,614 | 2,352 |
| **Average** | | | | 145 | 10,807 | 163 | 288 | 4,703 | 832 | 2,290 | 776 | 4,768 | 4,588 | 2,247 |
| | | | | | | | | | | | | | | |
| 3 | Al | 03/01/10 | 13:29 | 130 | 8,001 | 156 | 319 | 2,269 | 1,440 | 1,691 | 1,064 | 3,857 | 1,716 | 1,404 |
| 4 | Al | 02/26/10 | 8:48 | 143 | 6,881 | 157 | 286 | 1,650 | 1,241 | 1,308 | 1,053 | 2,938 | 1,580 | 1,133 |
| 8 | Al | 02/26/10 | 9:29 | 138 | 8,199 | 154 | 297 | 1,860 | 1,480 | 1,412 | 913 | 3,337 | 1,307 | 1,264 |
| 9 | Al | 03/01/10 | 14:02 | 155 | 6,560 | 160 | 292 | 1,848 | 1,130 | 2,902 | 804 | 3,077 | 1,762 | 2,894 |
| 9B | Al | 04/06/10 | | 137 | 9,445 | 154 | 307 | 2,149 | 1,445 | 1,154 | 2,875 | 3,892 | 1,820 | 846 |
| **Average** | | | | 141 | 7,817 | 156 | 300 | 1,955 | 1,347 | 1,693 | 1,342 | 3,420 | 1,637 | 1,508 |
| **Dual Simultaneous NSI Firings** | | | | | | | | | | | | | | |
| 6 | SS | 02/24/10 | 15:06 | 152 | 10,419 | 168 | 151 | 9,735 | 168 | ----- | ---- | 9,252 | 9,196 | ---- |
| 1 | Al | 03/01/10 | 14:43 | 149 | 6,456 | 164 | 149 | 6,244 | 163 | 719 | 10,210 | 4,863 | 4,857 | --- |
| | | | | | | | | | | | | | | |
| | | | **NOTES** | 1 | The pyrometer does not read temperatures below 572 °F | | | | | | | | | |
| | | | | 2 | "Side A" refers to the the fired side in a single NSI firing test; "Side B" is inert | | | | | | | | | |
| | | | | 3 | All times are measured from the start of the firing pulse (increase in amps) | | | | | | | | | |

The four single NSI firings with SS V-channel PCAs produced an average maximum temperature of 2,290 °F. In each test, the NSI produced a nearly circular hole punched or melted in the booster charge cover simulator, as shown in Figure 7.0-1.

*Figure 7.0-1. NSI Firings Run 2*

Five single NSI firings were conducted with Al Y-channel PCAs. One of the runs, Run 9, had a maximum temperature of 2,902 °F, which was much higher than any of the other run. Evidence of impact, external carbon deposits, and fractures in the sapphire window from this run led to suspicion that sealing arrangement leaked and the booster charge cover simulator may have been penetrated by particulate. Excluding this run gives an average maximum temperature of 1,391 °F for the remaining four Al Y-channel PCAs. All of the maximum temperatures were above 1,000 °F, which is the temperature judged to be sufficient to ignite the booster charge.

Figure 7.0-2 shows typical results for a representative single NSI firing in an Al Y-channel PCA. The pressure oscillations at the event start are due to the interaction of pressure transducer with the grease filled sense port channels. To estimate the true peak pressure for the test, a subset of the pressure data is used for a second order polynomial curve fit. The starting data point is determined using the value of the second pressure peak. Using this value, the pressure data earlier in the test is examined until a corresponding value is found. The subset ending data point is chosen where the pressure oscillations have dampened. This ending data point is at 800 μs after the trigger signal. The resulting second order polynomial curve-fit is then extrapolated to the intersection with the initial pressure rise curve. This intersection is the estimate of true peak pressure.

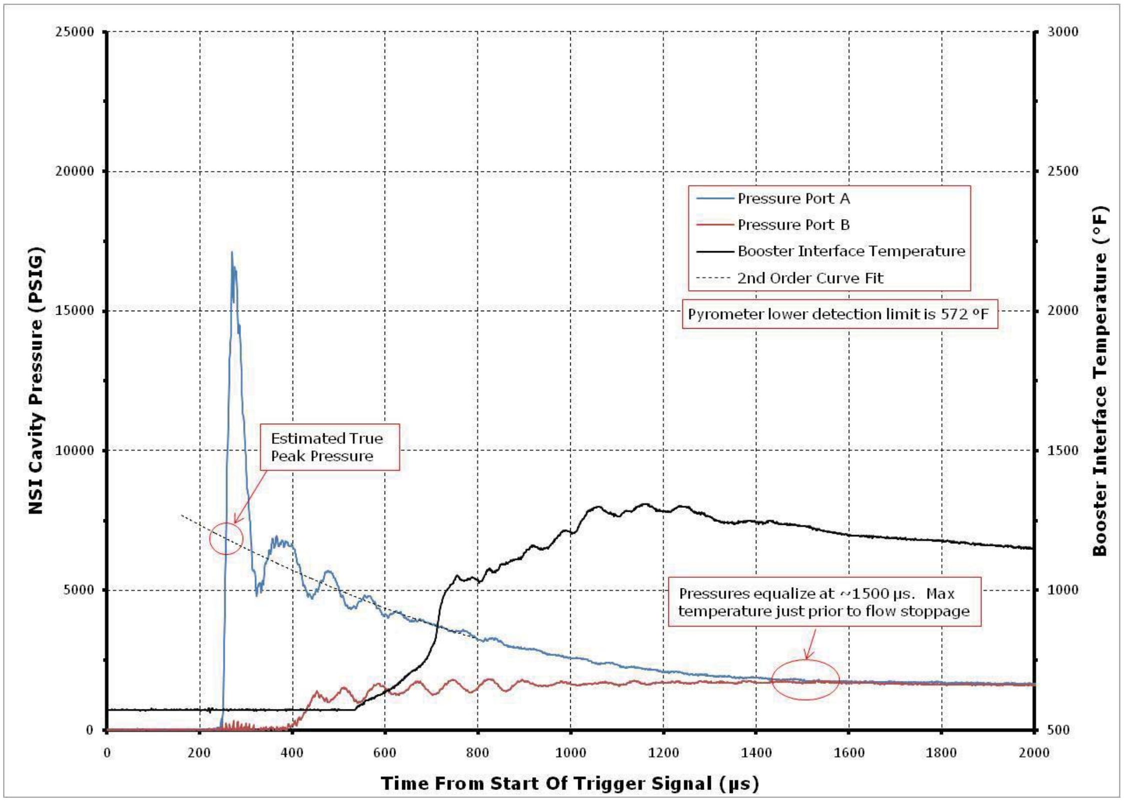


*Figure 7.0-2. Typical Results from a Single NSI Firing in an Al Y-Channel PCA (Run 4)*

As the NSI flow continues from the PCA active to the inactive side, the pressures begin to equalize. When the pressures equalize, there is no further driving force for flow. In this case, flow stopped about 1,300 µs after the initial 1,000 psig pressure rise. The maximum temperature at the booster interface occurs just prior to flow termination.

For comparison, Figure 7.0-3 shows typical results for a representative single NSI firing in a SS V-channel PCA.

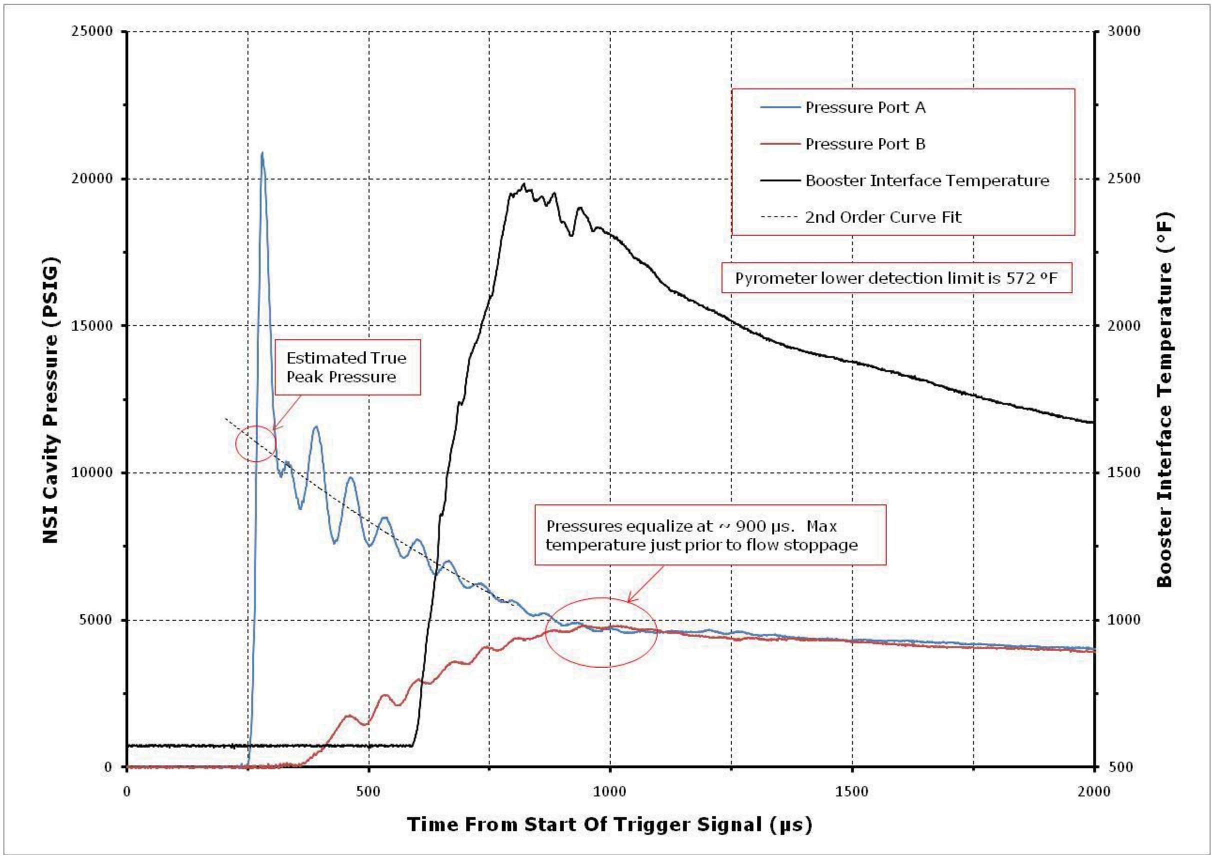


*Figure 7.0-3. Typical Results for a Single NSI firing in a SS V-Channel PCA (Run 15)*

In comparing Figures 7.0-2 and 7.0-3, it is evident the true peak pressure is higher (average 38 percent) with the SS than the Al PCA. Also, the pressure equalization and the maximum temperature occur earlier in the SS PCAs (i.e., 700 versus 1,300 µs). Since booster charge response was out of scope for this assessment and was not fired in this test series, further testing is needed to understand the effect the pressure difference would have on a pyrovalve function.

Figures 7.0-4 through 7.0-8 show the booster interface temperature results for Phase I tests. The Al Y-channel PCA results are shown by the black lines, while the SS V-channel PCA results are shown by the red lines. Figure 7.0-4 shows that the SS V-channel PCAs produce higher temperatures on average than the Al Y-channel PCAs. Figures 7.0-5 and 7.0-6 show the images obtained with the high-speed video (visual range) camera superimposed on a plot of the booster charge interface temperatures and NSI cavity pressures versus time.

Figure 7.0-7 shows the current traces for all the Phase I tests. As shown in the figure, this provides information about the timing of various events occurring in the test articles. Notice that the event timing is consistent in all the tests. This is partly due to the high firing current of 22 amps that was used to minimize any minor ignition differences in the NSIs.

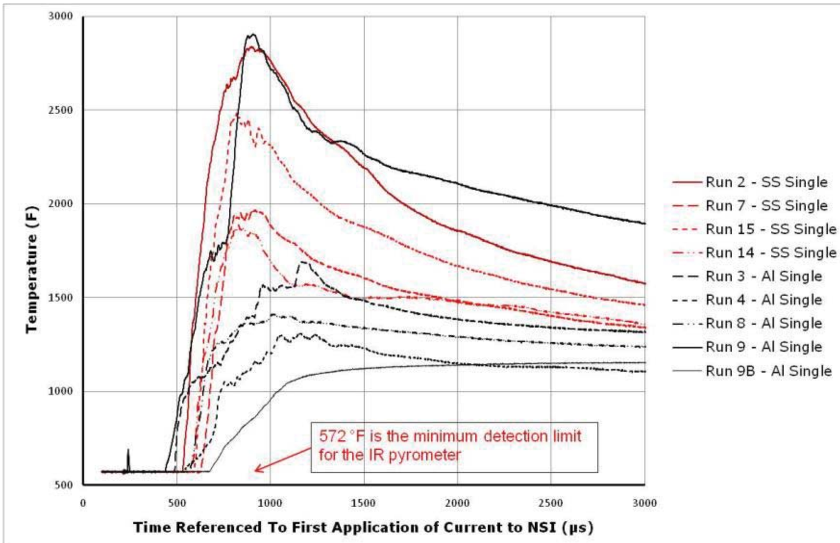


*Figure 7.0-4. Booster Propellant Interface Temperature Results for Phase I Tests*

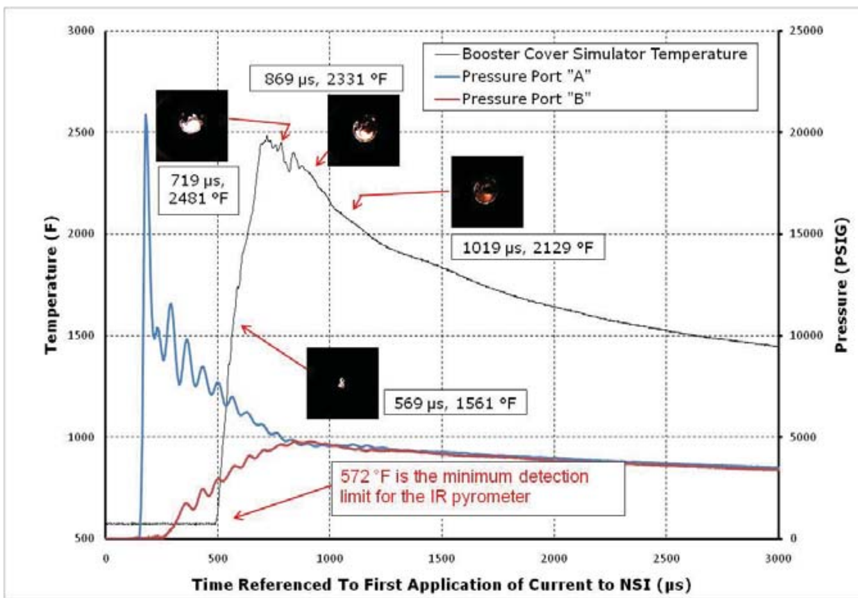


*Figure 7.0-5. Temperature and Pressures Versus Time for Phase I, Run 15, SS V-Channel PCA, Single NSI Firing*

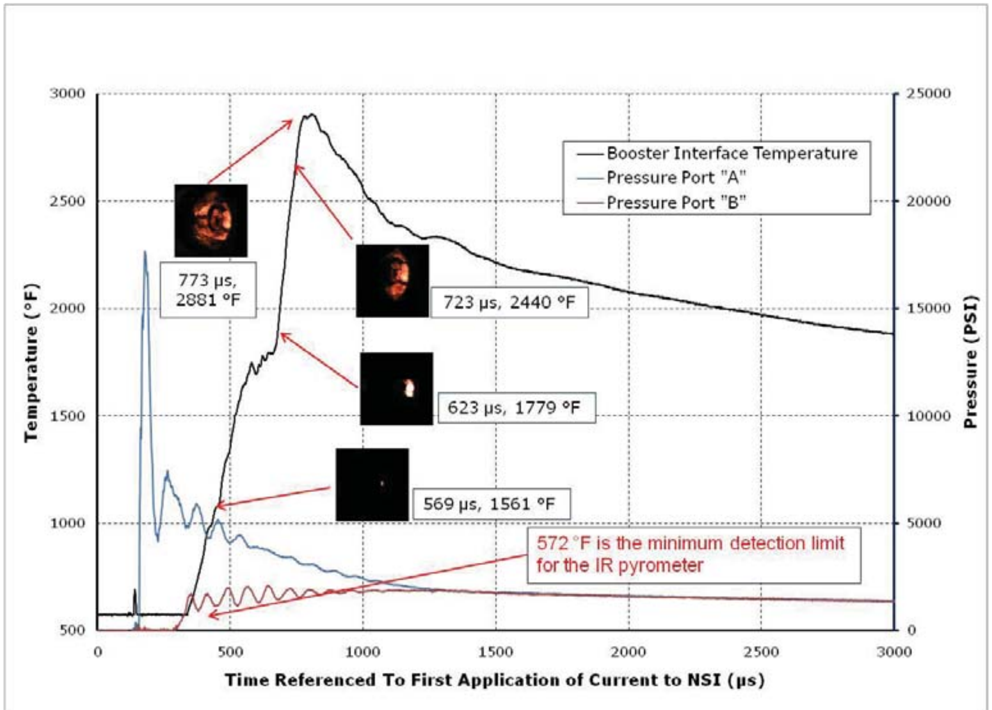


*Figure 7.0-6. Temperatures and Pressures for Phase I, Run 9, Al Y-Channel PCA, Single NSI Firing*

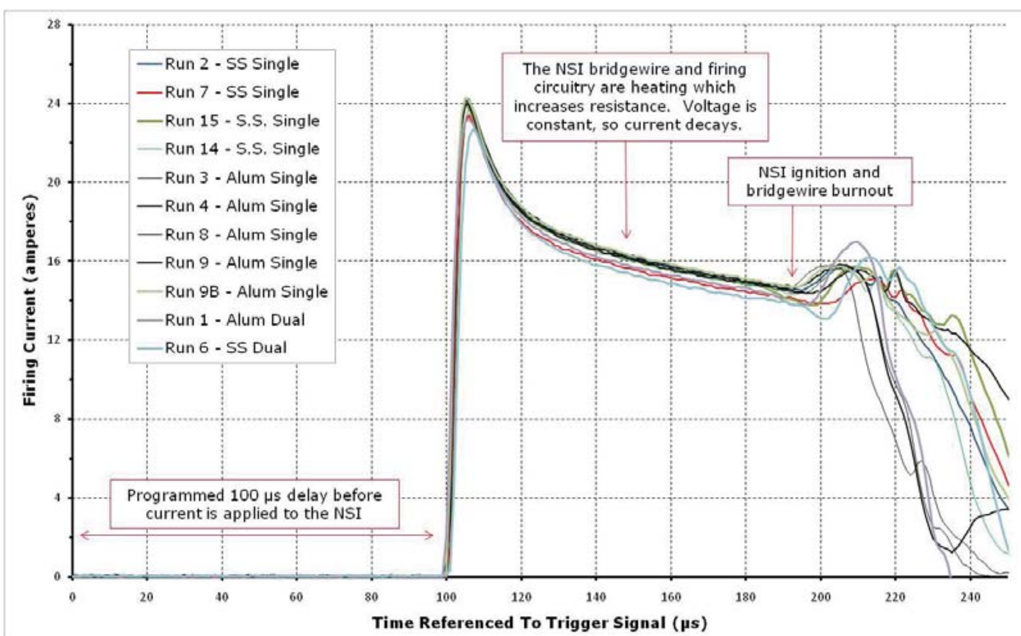


*Figure 7.0-7. NSI Current versus Time, Phase I*

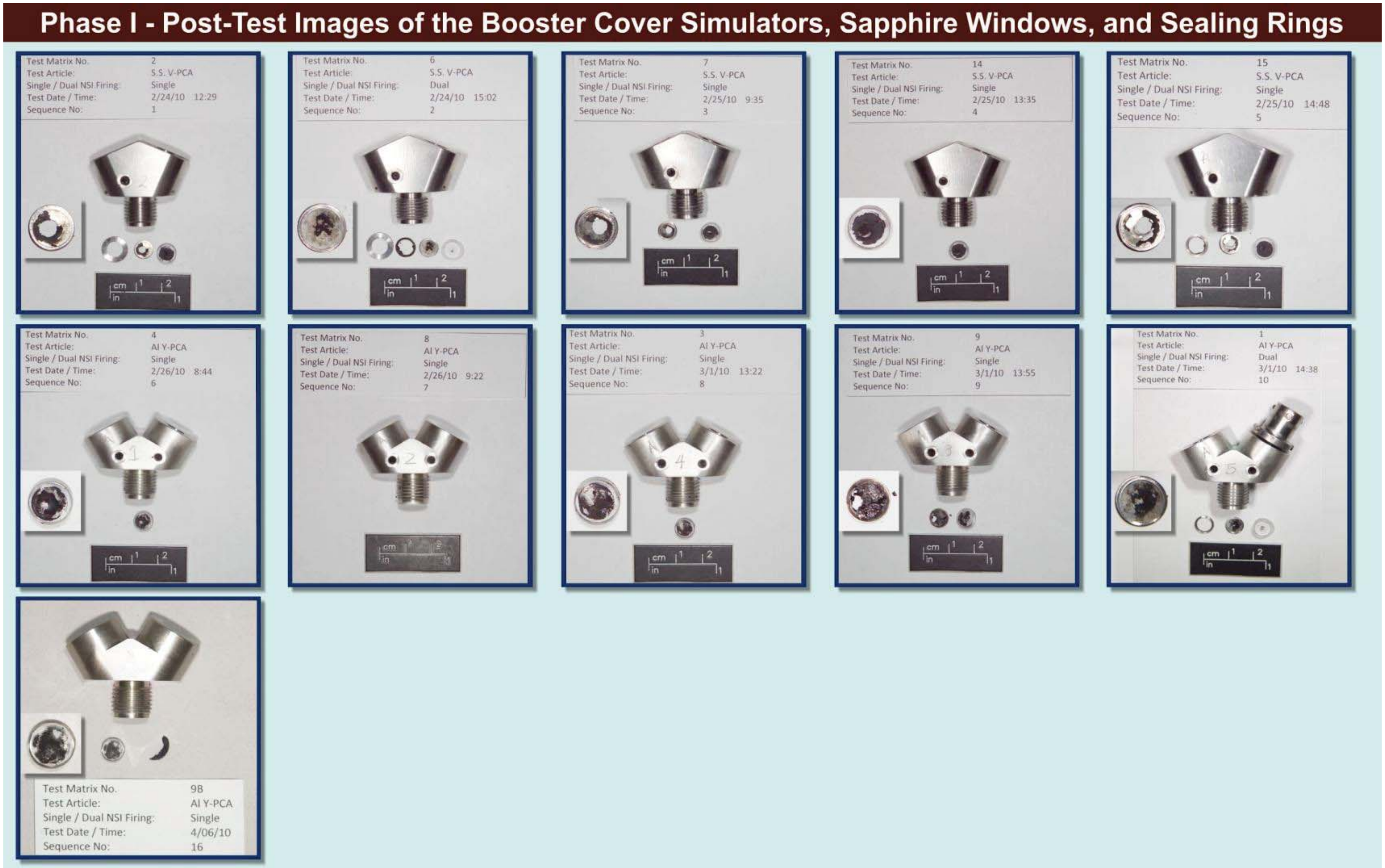


*Figure 7.0-8. Phase I- Post-Test Images of Booster Charge Cover Simulators, Sapphire Windows, and Sealing Rings*

*Table 7.0-2. Phase II Test Data Summary*

| Test Phase | Run No. | Channel Diameter (inch) | Actual Skew (µs) | Max Pressure Side A (psig) | Time Of Max Press Side A (µs) | Max Booster Interface Temp (°F) | Time Of Max Booster Interface Temp (µs) | Press Before Side B Rise (psig) | Max Pressure Side B (psig) | Time Of Max Press Side B (µs) |
|---|---|---|---|---|---|---|---|---|---|---|
| 2B | 1 | 0.060 | 6 | 10,437 | 225 | - | NA | NA | 9,781 | 235 |
| 2A | 3A | 0.060 | 16,000 | 9,641 | 224 | 3,410 | 16,434 | 1,574 | 13,039 | 16,057 |
| 2B | 4 | 0.060 | 486 | 11,389 | 224 | 2,913 | 1,132 | 2,532 | 15,076 | 713 |
| 2B | 5 | 0.060 | 485 | 10,780 | 220 | 3,078 | 1,161 | 5,661 | 15,371 | 710 |
| 2B | 7 | 0.060 | 5 | 9,715 | 223 | 1,723 | 217 | NA | 10,719 | 229 |
| 2B | 11 | 0.060 | 235 | 10,670 | 228 | 2,275 | 825 | 2,494 | 13,344 | 460 |
| Average | | | | 10,439 | 224 | 2,680 | 3,954 | 3,065 | 12,888 | 3,067 |
| 2A | 4 | 0.085 | 16,000 | 7,838 | 225 | 3,402 | 16,460 | 1,456 | 10,145 | 16,052 |
| 2B | 2B | 0.085 | 236 | 8,618 | 222 | 1,837 | 2,555 | 3,018 | 13,734 | 466 |
| 2B | 6A | 0.085 | 250 | 9,440 | 212 | 1,896 | 1,578 | 5,765 | 12,212 | 461 |
| 2B | 8 | 0.085 | 0 | 10,010 | 240 | 2,095 | 246 | NA | 10,477 | 240 |
| 2B | 13 | 0.085 | 237 | 9,017 | 219 | 1,733 | 1,208 | 3,208 | 14,220 | 459 |
| 2B | 9 | 0.085 | 242 | 8,493 | 222 | 2,517 | 965 | 3,140 | 13,094 | 461 |
| 2B | 14A | 0.085 | 8 | 9,637 | 224 | 1,723 | 220 | NA | 10,146 | 232 |
| 2B | 16 | 0.085 | 484 | 8,435 | 222 | 3,312 | 803 | 4,074 | 14,027 | 717 |
| 2B | 17 | 0.085 | 236 | 8,828 | 220 | 2,315 | 770 | 3,052 | 12,826 | 468 |
| Average | | | | 8,924 | 223 | 2,314 | 2,756 | 3,388 | 12,320 | 2,173 |
| 2A | 1A | 0.120 | 12 | 9,321 | 168 | - | NA | NA | 8,908 | 156 |
| 2A | 2 | 0.120 | 16,000 | 6,852 | 213 | 3,479 | 16,285 | 1,562 | 9,692 | 16,211 |
| 2B | 3A | 0.120 | 488 | 8,243 | 214 | 3,630 | 299 | 4,140 | 10,114 | 700 |
| 2B | 10 | 0.120 | 243 | 7,500 | 219 | 2,501 | 648 | 3,528 | 11,546 | 458 |
| 2B | 12 | 0.120 | 5 | 9,208 | 215 | 1,957 | 216 | NA | 9,785 | 221 |
| 2B | 14 | 0.120 | 484 | 7,208 | 219 | 3,630 | 774 | 3,528 | 10,389 | 706 |
| 2B | 15 | 0.120 | 5 | 9,161 | 222 | 699 | 3,700 | NA | 9,077 | 237 |
| Average | | | | 8,213 | 210 | 2,649 | 3,654 | 3,190 | 9,930 | 2,670 |

NOTES: All times are from the start of the firing signal
A red highlight indicates a temperature too low to ignite the booster propellant
A dash "-" indicates a temperature lower than the 572 °F lower limit detectable by the pyrometer
This means that the temperature could be anywhere between 72 °F and 572 °F

Phase II testing utilized SS V-channel PCAs and evaluated the effects of NSI skew and PCA flow passage cross-sectional area (Table 7.0-2). The SS V-channel PCAs were modified to have NSI flow passages with cross-sectional areas 2 and 4 times larger (0.085 and 0.120 inches, respectively) than the original design.

Phase IIA consisted of four tests. Tests were performed at each of the three different cross-sectional areas: nominal (Run 3A), 2 times the normal cross-sectional area (Run 4), and 4 times the normal cross-sectional area (Runs 1A and 2). To maximize the data obtained from each of these firings, the second NSI would be fired with a skew of 16,000 µs. The exception to this plan was Run 1A, which had a skew of 12 µs. The fourth test was to be a dual, simultaneous firing at the maximum cross-sectional area of 4 times the normal. Had this fourth test been successful in producing sufficient temperature at the booster interface, additional dual, simultaneous firing tests would be performed with the enlarged flow passages.

Figure 7-0.9 shows the NSI cavity pressure and the booster charge cover simulator temperature as a function of time. For Run 4, the flow passages were enlarged to twice the normal cross-sectional area. Both NSIs were fired in this test with a stagger time of 16,000 µs. It is evident in the figure that the PCA responded as if there were two separate NSI firings, each of which produced a maximum temperature in the 3,200 to 3,300 °F range. The three Phase IIA tests with NSI skew of 16,000 µs produced a maximum temperature at the booster interface ranging from 3,402 to 3,479 °F. Thus, there appears to be no practical benefit from enlarging the flow passages with a 16,000 µs skew as far as maximum booster interface temperature is concerned.

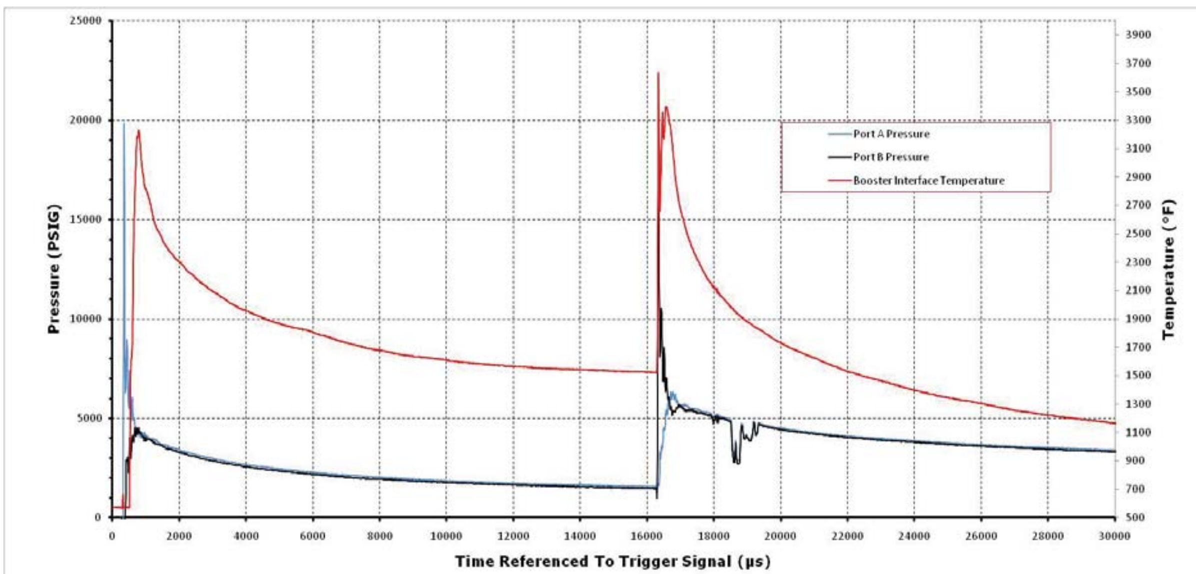


*Figure 7.0-9. Phase IIA Run 4*

Figure 7.0-10 shows the NSI cavity pressure and booster charge cover simulator temperature as a function of time. Run 1A was a dual, simultaneous firing with flow passages enlarged to 4 times the normal cross-sectional area. The skew in this test was 12 µs. As shown in the figure, there was no detectable increase in booster interface temperature. This means that the temperature was below the pyrometer lower temperature detection limit of 572 °F. This temperature is insufficient to ignite the booster propellant (i.e., approximately 1,000 °F). Therefore, even with enlarged flow passages with 4 times the normal cross-sectional area, dual, simultaneous firing remains a potential failure mode.

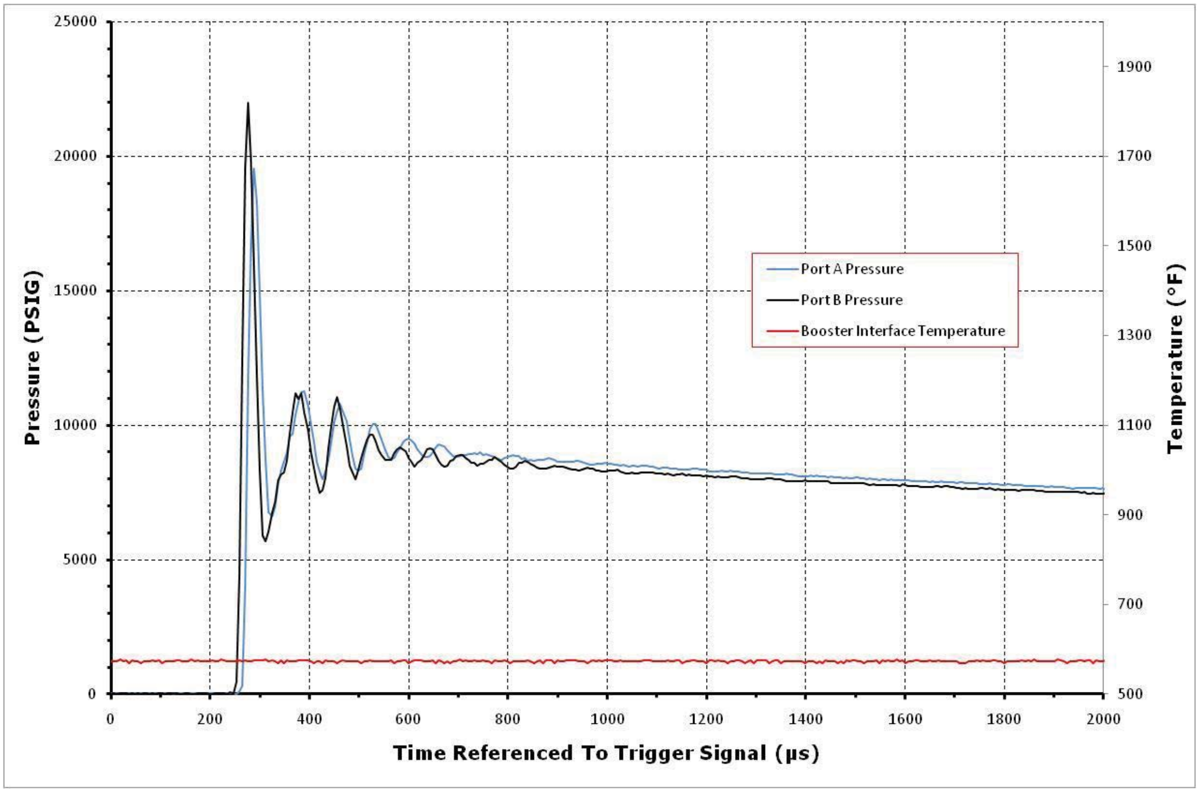


*Figure 7.0-10. Phase IIA, Run 1A*

In the majority of the Phase IIA tests, the pressure data went negative prior to the pressure rise (Figures 7.0-11 and 7.0-12). The negative values observed were approximately -500 psig. In these figures, the pressure scale is extended to -1,000 psig and the time scale expanded in the vicinity of the pressure rise from each of the two NSI firings.

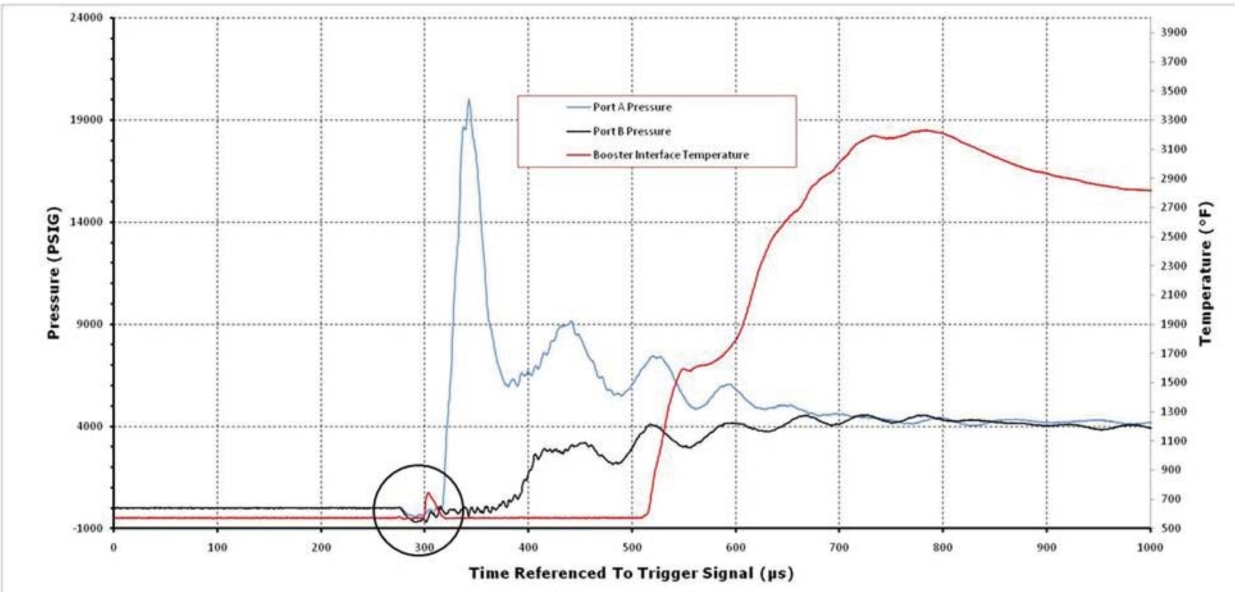


*Figure 7.0-11. Data from Phase IIA, Run 4 Showing the Negative Pressure Readings in the Vicinity of the First NSI Firing*

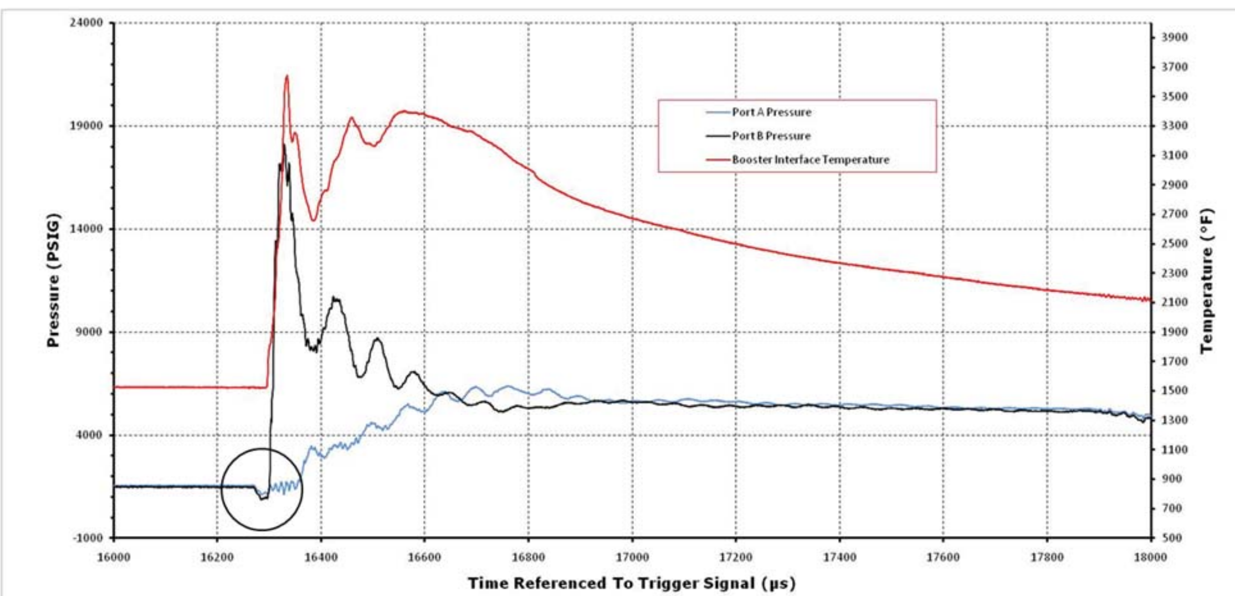


*Figure 7.0-12. Data from Phase IIA, Run 4 showing the Negative Pressure Readings in the Vicinity of the Second NSI Firing*

An investigation was performed to help understand why this occurred. This effect was not seen in instrumentation pre-test checkouts. These checkouts were performed routinely beginning with Phase IIB (Figure 7.0-13).

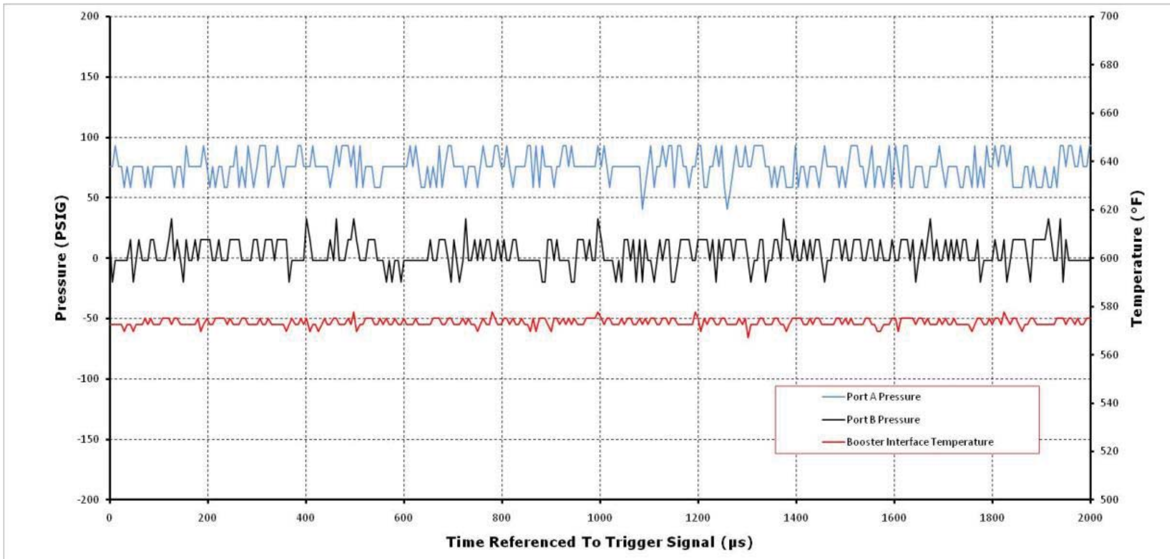


***Figure 7.0-13. Phase IIB, Run 1 Instrumentation Checkout Test shows No Negative Pressure Readings when Current is Applied to the NSI Simulators (Resistors)***

In these instrumentation checkouts, the test apparatus was configured identical to the planned PCA test. The only difference was that resistors are used to simulate the NSIs. In Figure 7.0-13, current is applied to the resistors 115 µs after the trigger signal. It is evident that there is no effect on either pressure or the temperature readings. Electrical effects from the plasma that is formed inside the NSI when the ZPP ignites may cause the negative pressure response. However, further investigation is required to determine the root cause. The testing continued at this point since the minor initial pressure dip did not appear to affect the data in the area of interest or change any conclusions.

Phase IIB continued to characterize the effects of skew and enlarged flow passages. Nominal skews of 5, 252.5, and 500 µs were tested with V-channel PCAs having flow passages with cross-sectional areas 1, 2, and 4 times that of the baseline design. The 5 µs skew was selected as a target to evaluate dual, simultaneous firing effects, while providing data at a skew greater than 0. Similarly, 500 µs was chosen to provide separation in firing times, while still evaluating possible interactions. The midpoint 252.5 µs and the 2 times the cross-sectional area were used so that a quadratic regression model could be fit to the data where necessary. This results approximately in a face-centered cubic efficient experimental design.

The flow paths with 2 and 4 times the cross-sectional area did not consistently produce greater temperatures at the booster interface. These cross-sectional areas did produce lower pressures in the NSI cavity (about 1,600 psi and 2,400 psi, respectively). This was not unexpected due to the larger free volume with enlarged flow paths.

Firings with attenuated temperatures and membrane burn-through percentages occurred predictably at nominally 0 skew. Figure 7.0-14 shows the images captured from a high-speed video camera aimed at the underside of the booster charge cover simulator. In each case, the image was selected to illustrate the maximum effect on the simulator (Table 7.0-3). Note that because the simulator is an opaque metal disk, combustion gases and particles are only visible following disk penetration.

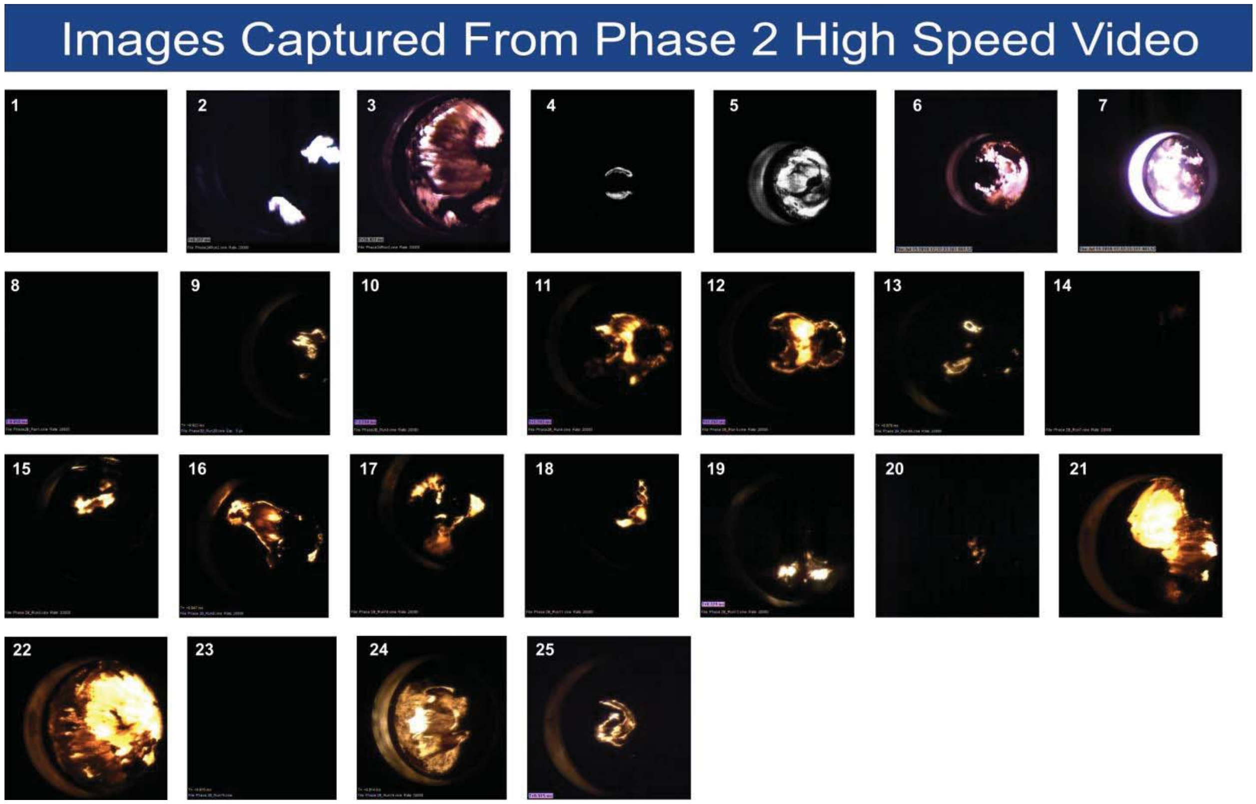


*Figure 7.0-14. Images Captured from Phase II High-Speed Video Camera*

*Table 7.0-3. Phase II High-Speed Video Data Summary*

| Image No. | Phase | Run No. | Channel Dia (in) | Skew (μs) |
|---|---|---|---|---|
| 1 | 2A | 1A | 0.120 | 12 |
| 2 | 2A | 2 | 0.120 | 16000 |
| 3 | 2A | 2 | 0.120 | 16000 |
| 4 | 2A | 3A | 0.06 | 16000 |
| 5 | 2A | 3A | 0.06 | 16000 |
| 6 | 2A | 4 | 0.085 | 16000 |
| 7 | 2A | 4 | 0.085 | 16000 |
| 8 | 2B | 1 | 0.06 | 6 |
| 9 | 2B | 2B | 0.085 | 236 |
| 10 | 2B | 3 | 0.120 | 481 |
| 11 | 2B | 4 | 0.06 | 486 |
| 12 | 2B | 5 | 0.06 | 485 |
| 13 | 2B | 6A | 0.085 | 250 |
| 14 | 2B | 7 | 0.06 | 5 |
| 15 | 2B | 8 | 0.085 | 0 |
| 16 | 2B | 9 | 0.085 | 242 |
| 17 | 2B | 10 | 0.120 | 243 |
| 18 | 2B | 11 | 0.06 | 235 |
| 19 | 2B | 12 | 0.120 | 5 |
| 20 | 2B | 13 | 0.085 | 237 |
| 21 | 2B | 14 | 0.120 | 484 |
| 22 | 2B | 14 | 0.120 | 484 |
| 23 | 2B | 15 | 0.120 | 5 |
| 24 | 2B | 16 | 0.085 | 484 |
| 25 | 2B | 17 | 0.085 | 236 |

## 7.1 Modified SS V-Channel PCA Test

To supplement this study, computational fluid dynamics (CFD) modeling was performed by Craftech® (reference Section 7.5 and Volume II, Appendix E). The work was performed under NASA Phase I Small Business Innovation Research (SBIR) Topic No. X2.01-9934, "Design

Support and Analysis Tool for Pyrotechnically Actuated Valves," Contract No. NNX11CG13P, Report No. 01/C472. The CFD modeling indicated that chambers machined adjacent to the flow channels reduced the tendency toward the stagnation condition that caused low booster interface temperatures during simultaneous firings. This was thought to have the potential for eliminating the requirement for minimum skew. A SS V-channel PCA with the normal 0.060-inch diameter flow channels was modified to have two resonant chambers (total volume 0.00789 $in^3$) as shown in Figure 7.1-1.

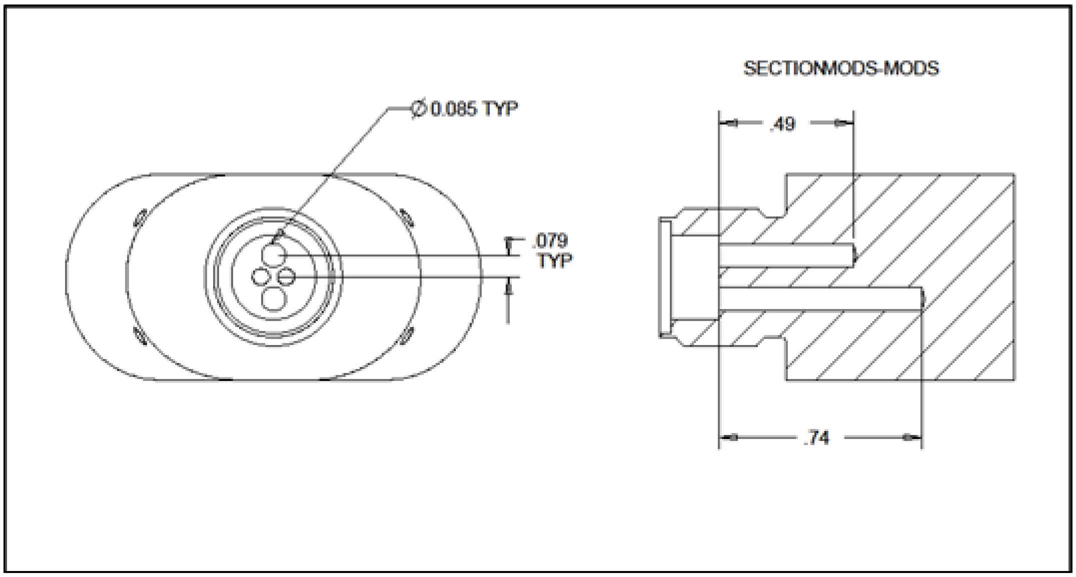


*Figure 7.1-1. SS V-Channel PCA Modified With Two Resonant Chambers*

To investigate the CFD analysis, a special dual, simultaneous NSI firing (5 µs skew) test was performed (Figure 7.1-3). Phase IIB Run 1 data is plotted for comparison. The maximum temperature on Run 1 was below the minimum detectable limit of the pyrometer (572 °F). The maximum temperature on the resonant chamber test was 782 °F, which is below the minimum temperature of 1,000 °F to ignite the booster charge. Therefore, this specific resonant chamber modification did not eliminate the potential failure mode resulting from the dual, simultaneous NSI firing. This investigation was proof of concept only, and not intended to be a rigorous examination of resonant chamber volume versus PCS design and NSI skew.

Figure 7.1-2 is a photograph of the modified V-channel PCA showing the location of the two resonant chambers.

*Figure 7.1-2. SS V-Channel PCA with Two Resonant Chambers*

The new chambers are the larger diameter holes. The smaller holes are the normal 0.060-inch diameter flow channels from the NSIs.

A dual, simultaneous NSI test firing was performed with this test article. The results are shown in Figure 7.1-3. Phase IIB Run 1 data is plotted on the same graph for comparison. Both were dual, simultaneous firings with nominal (0.060-inch diameter) flow passages and 6 μs skew. The maximum temperature on Run 1 was below the minimum detectable limit of the pyrometer (572 °F). The maximum temperature on the resonant chamber test was 782 °F. Previous test work has shown that in this rapid temperature rise situation, 1,000 to 1,100 °F is needed to ignite the booster. Therefore, this specific modification did not eliminate the potential failure mode resulting from the dual, simultaneous NSI firing. However, the added 0.00789-cubic-inch volume was less than what was modeled and due to budget limitations, testing was not done with larger added volumes. The NESC, or future programs considering applying the modification, would need to plan on additional testing.

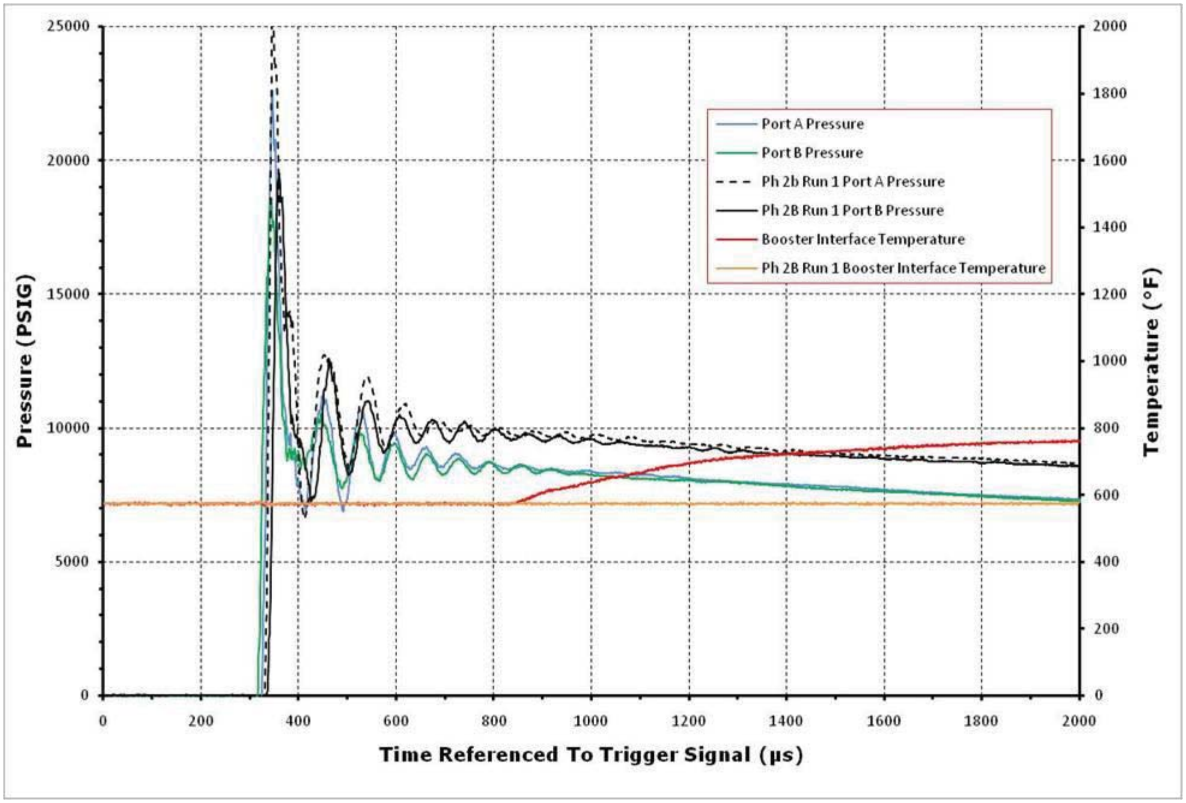


*Figure 7.1-3. Comparison of a Dual, Simultaneous NSI Firing With and Without a Modified SS V-Channel PCA*

Post-test examination revealed little damage to the booster charge cover simulator, which is consistent with other dual, simultaneous NSI firing tests where the membrane is not breached. See Figure 7.1-4.

*Figure 7.1-4. Sealing Ring, Sapphire Window, and Booster Charge Cover Simulator from the Modified SS V-Channel PCA*

## 7.2 PCA Thermal Analysis

To quantify the contribution of various heat transfer mechanisms in the booster charge cover thermal response, simplified and detailed thermal analyses were performed. These analyses are provided in Appendix E, with conclusions summarized in the following section.

### 7.2.1 Conclusions

Three heat transfer mechanisms and their effect on booster cap thermal response were investigated as part of this study. From the analysis, the following conclusions are drawn:

a. Convective heat transfer, by itself, may not account for the temperature rise and melting during booster cap testing. Further computational and/or empirical quantification of gas temperatures and heat transfer coefficients are needed to draw a definitive conclusion as to whether convection alone is sufficient.

b. Zirconia deposition and the subsequent phase change from the liquid to solid state may assist in booster cap heating and subsequent melting but does not produce booster cap temperatures in agreement with the booster cap transient temperature response observed during testing. Larger quantities of zirconia deposition increase the propensity to melt and accelerate the temperature rise of the booster cap bottom.

c. Unburned ZPP deposition can liberate sufficient energy to locally melt through the booster cap as indicated by detailed thermal analysis of a hemispherical globule of ZPP with a radius of $3.6\times10^{-3}$ in with a mass of $5.2\times10^{-3}$ mg ($1.14\times10^{-8}$ lbm). Deposition of as little as 20 percent of the unburned ZPP (~4.6 mg, or $1\times10^{-5}$ lbm) can liberate sufficient energy to melt the entire booster cap. Subsequent two-dimensional axisymmetric thermal analysis shows that local melt-through can be accomplished with considerably less ZPP. From this, it is concluded that << 4.6 mg ZPP burning in contact with the booster cap is sufficient to produce the observed response.

While heat transferred by convection and by the phase change of liquid zirconia deposited on the booster cover simulator, the unburned ZPP results are a compelling indication that this mechanism could be a viable alternative mechanism. There would presumably be a lot of variation in the quantity, size and impingement locations of unburned ZPP that could explain inconsistent performance of the NSIs.

## 7.3 Phases I and II Statistical Analysis

This section provides a summarization of the statistical analysis and results from the Phase I and Phase II testing. More complete analysis information is provided in Volume II, Appendices F and G.

Phases I and IIB were conducted using DOE principles:

1. A clear statement of the problem was developed for each phase. The problem statements were testable, of defined scope, and agreed upon by the entire assessment team.
2. Factors (inputs) and responses (outputs) were quantifiable, tractable, and measurable.
3. The domains over which the factors would be varied were broad enough to be able to discern in outputs, if they existed, and addressed the statements of problem.
4. The test matrices were defined taking these points into account and so the data would be analyzable, resulting in clear conclusions on which to base recommendations. The test matrices were to include randomization to ensure independence of data and minimize issues due to special causes, minimum correlation between factors (orthogonality) to ensure that the factors' effects on the responses could be separated ensuring that there existed analysis methods to examine the data and other efficiencies.
5. Analysis of variance (ANOVA) and similar firmly-based methods were employed in the analysis.

Most of these principles were followed. However, randomization was not fully performed, but the assessment team feels this did not seriously compromise the investigation conclusions. The assessment team generated robust experiments and the analysis results are clear in most cases. In the cases where they are not, it is concluded that this was not due to the experimental design, but rather to the phenomena tested being noisy and/ or there being little effect on the responses by these factors.

Phase I was designed to quantify the difference between the Al Y-channel and SS V-channel PCAs in temperature measured at the simulated booster charge cover and in pressure in various parts of the system. It was also meant to, at a minimum, qualitatively and better quantitatively characterizes what happens at 0 skew time conditions and provides an idea of the range of response values to help design follow-on tests.

All these goals were met. The two simultaneous firings showed less-desirable temperature responses than the single firings, and could have produced a no-fire condition. Analysis produced expected values (means) for a number of responses. Temperatures were both statistically and engineering-wise significantly higher for the SS runs than for the Al runs. Key pressure measurements were significantly higher for the SS runs in both statistical and engineering terms.

***Table 7.3-1. Summary Table of Response Means and 95 Percent Confidence Intervals on the Means***

| **Response** | **SS Mean** | **± 95 percent** | **Al Mean** | **± 95 percent** | **Notes** |
|---|---|---|---|---|---|
| Time of Maximum Temperature | 776 | 120 | 959 | 120 | |
| Peak Temperature | 2,290 °F | 431 | 1,391 °F | 431 | Ignored Run 9 |
| Temperature at 800 µs | 2,247 °F | 440 | 1,162 °F | 440 | Ignored Run 9 |
| Time of Port A Pressure Rise Start | 144 µs | 5 | 137 µs | 5 | Ignored Run 9; included duals |
| Port A Calculated Peak Pressure | 10,729 psi | 289 | 7,796 psi | 1,292 | Ignored Run 9; included duals; weighted analysis |
| Port A Pressure at 800 µs | 4,768 psi | 406 | 3,420 psi | 363 | |
| Time of Port B Pressure Rise Start | ~295 µs | | ~295 µs | | Difference not significant |
| Port B Calculated Peak Pressure | 4,779 psi | 313 | 1,895 psi | 283 | Included Duals |
| Port B Time to Peak Pressure | ~830 µs | | ~1,400 µs | | Runs 9 and 9B may be outliers |
| Port B Pressure at 800 µs | 4,588 psi | 300 | 1,637 psi | 269 | |

Phase IIB was designed to evaluate the relationship between firing skew time and flow passage cross-sectional area. It was assumed that the following model could be used to describe these relationships:

$$Y = \beta_0 + \beta_1 \text{ Skew} + \beta_2 \text{ Area} + \beta_{12} \text{ Skew x Area} + \beta_{11} \text{ Skew}^2 + \beta_{22} \text{ Area}^2$$

where the β's are linear regression parameters fit using the data and Y could represent any of the chosen response variables.

Test results showed that within the tested range of flow passage area, a no-fire is likely to occur given near-simultaneous firings. The test was not designed to characterize the risk of no-fire with skew time. The assessment team cannot determine that the chance of a no-fire does or does not decrease to a negligible level at 500 µs skew given this data alone.

Analyses included characterization of a response surface for most output variables. Some are notional, and involve extrapolations in the area of 0 skew. Others appear to characterize the behavior of the responses adequately over the input factors' domain. The assessment team performed a single confirmation run that could not be shown to invalidate the model predictions. The assessment team did not perform confirmation runs. The assessment team is satisfied the qualitative and quantitative conclusions are adequately supported by the data.

Booster charge cover temperature, both peak and 1,600 µs after NSI ignition, depends statistically significantly on skew time, but not on flow passage cross-sectional area. The time to attain 1,000 °F at the Booster cover was not found to be statistically significantly predicted by skew of flow passage cross-sectional area. There were indications that another, unmeasured variable could have affected this measure.

Pressures after the initial NSI firing were statistically significantly depressed by a combination of high skew time and high flow passage cross-sectional area. Longer skews promoted higher pressures after the second NSI initiation, but larger channel area diminished peak pressure after the second initiator firing. Pressure at 1,600 µs was statistically significantly lessened in high-passage cross-section area runs compared with low-area runs, but was not significantly affected by skew.

Measurements and analysis of the booster charge cover hole size were problematic. Near 0-skew runs showed no burn-through. It appears reasonable that the data shows that higher skews correspond to larger burn-through areas, but flow passage cross-sectional area may not affect this.

## 7.4 Numerical Simulations of Single and Simultaneous Dual Firing Initiators in the SS V-Channel PCA Design[2]

In addition to the PCA thermal analysis discussed in Section 7.2, SS PCA numerical simulations (computer modeling) were accomplished by Craftech® under the SBIR program, in collaboration with this project. Details of this modeling are provided in Volume II, Appendix H. This numerical modeling effort, based on CFD modeling, provided an improved understanding of the gas and particle flow physics within the V-channel PCA. One of the primary issues explored by this test project, the dual simultaneous NSI ignition anomaly was explained as interaction of the shocks formed by the two NSIs and stagnation at the booster interface. The stagnation condition and reflected waives appeared to reduce the amount of ZPP particles (hot burning) from reaching the booster membrane, causing the membrane temperature to be dramatically lower. Modeling of a modified V-channel PCA with additional chambers either side of the flow channels also accomplished as discussed Section 7.1.

[2] Ashvin Hosangadi, Jai Sachdev, and Roger Birkbeck, Combustion Research and Flow Technology, Inc. (Craftech®)

# 8.0 Findings, Observations, and NESC Recommendations

## 8.1 Findings

The following findings were identified:

**F-1.** The SS V-channel PCA units delivered improved performance in the following areas:

a. An average maximum booster/propellant interface temperature approximately 600 °F greater than that delivered by the Al Y-channel PCA units.

b. The SS V-channel PCAs delivered higher temperatures to the booster interface providing added assurance of booster propellant ignition (refer to Table 7.0-1).

c. The higher temperatures with the SS V-channel PCAs were achieved in approximately one-half the time; 776 µs average for the SS V-channel PCAs versus 1,342 µs average for the Al Y-channel PCAs.

d. The SS V-channel PCAs produced pressures in the NSI cavity that were approximately 3,000 psi greater than the Al Y-channel PCAs.

**F-2.** The tests showed that dual, simultaneous firing of the redundant NSIs significantly reduces the performance of not only the Al Y-channel PCA design as found previously, but also the SS V-channel PCA design to the point where it is doubtful the booster charge would be reliably ignited. The threshold for "no fire" may be higher than 20 µs skew, but no failures were observed at 250 µs skew and higher. This testing was not designed to determine a relationship between skew and ignition reliability parametrically. The bounds of effects due to 'simultaneous firing', therefore, almost certainly lie above 20 µs and may be above 250 µs.

a. The booster interface temperature needed to ignite the titanium hydride/potassium perchlorate booster charge is approximately 1,000 °F under rapid rise conditions present in the booster.

b. In about 50 percent of the dual, simultaneous test firings the maximum temperature observed was below or just slightly above the lower limit of 572 °F that could be detected by the test instrumentation.

**F-3.** Enlarging the flow passages, even up to 4 times nominal cross-section, did not mitigate the risk of unreliable booster charge ignition from dual simultaneous firings of redundant NSIs.

**F-4.** The assessment did not show consistently greater temperatures with larger NSI flow channels at the booster interface.

## 8.2 Observations

The following observations were identified:

**O-1.** When the flow path diameter and the skew are high, they exert a considerable downward effect on peak pressure.

a. The flow paths with cross-sectional areas 2 and 4 times greater than the original design produced lower pressures in the NSI cavity.

b. The reduction was about 1,600 psi and 2,400 psi, respectively.

c. This was not unexpected due to the obviously larger free volume with the enlarged flow paths.

**O-2.** Increasing the flow passage diameter from the original 0.060-in diameter to 0.120-in (4 times the original cross-sectional area) lowers the maximum pressure inside of the PCA by about 2,000 psi or about 21 percent.

**O-3.** SS PCA modeling suggested that additional chambers machined into the PCA might preclude the stagnation condition and mitigate the anomaly. Fully exploring this mitigation was beyond the scope of this assessment.

**O-4.** A new and innovative temperature measurement method was developed and used for this assessment that is accurate to within 50 °F over a range of 572 to 3,632 °F and has a rapid response time of 10 μs or less.

## 8.3 NESC Recommendations

The following NESC recommendations are directed at the NASA Programs and Projects using PCAs:

**R-1.** Ensure that NSI firing circuits are characterized under as-built design and all mission conditions to determine the effective NSI firing skew time, and implement a commanded firing time of dual NSI PCAs that is longer than this value. ***(F2)***

- MSL testing determined ignition capability/margin was 8 ms, and implemented a minimum skew of 16 ms.

**R-2.** Use SS V-channel in preference to Al Y-channel PCAs due to their increased capability to reliably activate the booster charge. ***(F-1)***

**R-3.** Explore the merit of resonant chambers to determine if this design feature eliminates the requirement for a minimum NSI skew time. ***(O-4)***

# 9.0 Alternate Viewpoints

There were no alternate viewpoints identified during the course of this assessment by the NESC team or the NRB quorum.

## 10.0 Other Deliverables

No unique hardware, software, or data packages, outside those contained in this report, were disseminated to other parties outside this assessment.

## 11.0 Lessons Learned

No applicable lessons learned were identified for entry into the NASA Lessons Learned Information System (LLIS).

## 12.0 Definition of Terms

| | |
|---|---|
| Corrective Actions | Changes to design processes, work instructions, workmanship practices, training, inspections, tests, procedures, specifications, drawings, tools, equipment, facilities, resources, or material that result in preventing, minimizing, or limiting the potential for recurrence of a problem. |
| Finding | A conclusion based on facts established by the investigating authority. |
| Lessons Learned | Knowledge or understanding gained by experience. The experience may be positive, as in a successful test or mission, or negative, as in a mishap or failure. A lesson must be significant in that it has real or assumed impact on operations; valid in that it is factually and technically correct; and applicable in that it identifies a specific design, process, or decision that reduces or limits the potential for failures and mishaps, or reinforces a positive result. |
| Observation | A factor, event, or circumstance identified during the assessment that did not contribute to the problem, but if left uncorrected has the potential to cause a mishap, injury, or increase the severity should a mishap occur. Alternatively, an observation could be a positive acknowledgement of a Center/Program/Project/Organization's operational structure, tools, and/or support provided. |
| Problem | The subject of the independent technical assessment. |
| Proximate Cause | The event(s) that occurred, including any condition(s) that existed immediately before the undesired outcome, directly resulted in its occurrence and, if eliminated or modified, would have prevented the undesired outcome. |
| Recommendation | An action identified by the NESC to correct a root cause or deficiency identified during the investigation. The recommendations may be used by |

| | |
|---|---|
| | the responsible Center/Program/Project/Organization in the preparation of a corrective action plan. |
| Root Cause | One of multiple factors (events, conditions, or organizational factors) that contributed to or created the proximate cause and subsequent undesired outcome and, if eliminated or modified, would have prevented the undesired outcome. Typically, multiple root causes contribute to an undesired outcome. |

# 13.0 Acronyms List

| | |
|---|---|
| Al | Aluminum |
| ANOVA | Analysis of variance |
| Btu | basic terminal unit |
| CAD | computer-aided design |
| CFD | computational fluid dynamics |
| DOE | design of experiments |
| DPIC | Dual Pyrovalve Initiator Circuit |
| GSFC | Goddard Space Flight Center |
| IR | Infrared |
| JPL | Jet Propulsion Laboratory |
| L/D | Ratio of length to diameter |
| LaRC | Langley Research Center |
| $lb_f$ | pounds per force |
| lbm | pounds mass |
| MPCV | Multi-Purpose Crew Module |
| MSFC | Marshall Space Flight Center |
| MSL | Mars Science Laboratory |
| MTSO | Management and Technical Support Office |
| NESC | NASA Engineering and Safety Center |
| NRB | NESC Review Board |
| NSI | NASA Standard Initiators |
| PCA | Primer Chamber Assembly |
| SBIR | Small Business Innovation Research |
| SLS | Space Launch System |
| SS | stainless steel |
| THPP | Titanium Hydride Potassium Perchlorate |
| VDC | voltage direct current |
| WSTF | White Sands Test Facility |
| ZPP | zirconium potassium perchlorate |
| $ZrO_2$ | zirconium oxide |

# 14.0 References

1. Hagopian, Michael and Dibbern, Andreas, Conax Pyrotechnic Valve Failures Investigation, NASA/TM-20008-215548 (NESC-RP-08-111/06-009-E), October 30, 2008.
2. Lee, H.S., Estimating Heat Losses in Pyrotechnic Devices, AIAA-2005-3837, July 2005.
3. http://www.americanelements.com/zrox.html.
4. Sharafat, S., Kobayashi, A., Ogden, V., and Ghoniem, N., Development of Composite Thermal Barrier Coatings with Anisotropic Microstructure, Vacuum 59 (2000), pp. 185-193, Pergamon.
5. CAD file: Alum 1125-279-04.stp.
6. Computer File: NSI-29_No_Filter_V1_0.avi.
7. MCDOUGLE_PHOTO Model(1).pdf.

## Volume II: Appendices (separate volume)

# REPORT DOCUMENTATION PAGE

*Form Approved*
*OMB No. 0704-0188*



| 1. REPORT DATE *(DD-MM-YYYY)* | 2. REPORT TYPE | 3. DATES COVERED *(From - To)* |
|---|---|---|
| 01- 10 - 2011 | Technical Memorandum | November 2009 - July 2011 |

**4. TITLE AND SUBTITLE**
Comparison of the Booster Interface Temperature in Stainless Steel (SS) V-Channel versus the Aluminum (Al) Y-Channel Primer Chamber Assemblies (PCAs)

**5a. CONTRACT NUMBER**

**5b. GRANT NUMBER**

**5c. PROGRAM ELEMENT NUMBER**

**6. AUTHOR(S)**
Garcia, Roberto; Saulsberry, Regor L.

**5d. PROJECT NUMBER**

**5e. TASK NUMBER**

**5f. WORK UNIT NUMBER**
869021.05.07.01.10

**7. PERFORMING ORGANIZATION NAME(S) AND ADDRESS(ES)**
NASA Langley Research Center
Hampton, VA 23681-2199

**8. PERFORMING ORGANIZATION REPORT NUMBER**
L-20081 NESC-RP-09-00596

**9. SPONSORING/MONITORING AGENCY NAME(S) AND ADDRESS(ES)**
National Aeronautics and Space Administration
Washington, DC 20546-0001

**10. SPONSOR/MONITOR'S ACRONYM(S)**
NASA

**11. SPONSOR/MONITOR'S REPORT NUMBER(S)**
NASA/TM-2011-217182/Volume I

**12. DISTRIBUTION/AVAILABILITY STATEMENT**
Unclassified - Unlimited
Subject Category 20 Spacecraft Propulsion and Power
Availability: NASA CASI (443) 757-5802

**13. SUPPLEMENTARY NOTES**

**14. ABSTRACT**
NASA's Technical Fellow for Propulsion, requested a technical assessment of the performance improvement achieved by the introduction of the stainless steel (SS) V-channel compared to the aluminum (Al) Y-channel Primer Chamber Assembly (PCA) design. The SS V-channel PCA was developed for NASA's Mars Science Laboratory (MSL) Project. The principle focus of the assessment was to measure the transient temperature at the booster interface with both designs. This document contains the findings of the assessment.

**15. SUBJECT TERMS**
Primer Chamber Assembly; NASA Engineering and Safety Center; Pyrovalve Booster; Dual Pyrovalve Initiator Circuit

| 16. SECURITY CLASSIFICATION OF: | | | 17. LIMITATION OF ABSTRACT | 18. NUMBER OF PAGES | 19a. NAME OF RESPONSIBLE PERSON |
|---|---|---|---|---|---|
| a. REPORT | b. ABSTRACT | c. THIS PAGE | | | STI Help Desk (email: help@sti.nasa.gov) |
| | | | | | 19b. TELEPHONE NUMBER *(Include area code)* |
| U | U | U | UU | 55 | (443) 757-5802 |

**Standard Form 298** (Rev. 8-98)
Prescribed by ANSI Std. Z39.18